UHS Relay Testing for Optimal Protection of a Long 345 kV Line With Series Compensation

Matthew J. Lewis, *Lone Star Transmission, LLC*
Faris M. Elhaj, *OMICRON electronics Corp.*
Richard D. Kirby, *Schweitzer Engineering Laboratories, Inc.*

Abstract—This paper focuses on testing and field experience with ultra-high-speed (UHS) line protective relays at Lone Star Transmission, LLC (Lone Star). The 345 kV transmission corridor at Lone Star comprises two series-compensated lines: 224.9 mi and 189.6 mi. These lines share the same series-compensation sites and include shunt reactors at one of the capacitor locations. The series-compensation substations do not have circuit breakers, and therefore you cannot split the line into selective protection zones. Instead, Lone Star uses transfer tripping to trip the entire line for faults at the compensation substations. As a result, the protection is complex, and accurately locating faults can be difficult with phasor-based impedance and line current differential protection. In 2019, Lone Star installed four UHS relays that use principles based on incremental quantities and traveling waves.

This paper discusses a system-based testing approach for verifying the performance of these UHS relays. It explains a simulation testing software model and the variety of operational scenarios we simulated to improve Lone Star's protection philosophy for series-compensated transmission lines in the future. The paper includes the results from these tests, the related optimization of the UHS relay settings, and an evaluation of the UHS-based protection scheme performance for three field events.

I. INTRODUCTION AND SYSTEM OVERVIEW

Lone Star Transmission, LLC (Lone Star) is a transmission owner and operator in North Texas. Initially, they were a transmission provider as part of the ERCOT Competitive Renewable Energy Zones (CREZ) transmission buildout in 2011 to transport surplus west Texas electricity to loads in northeast Texas. The CREZ initiative was mandated by the Texas legislature to strengthen the power grid and enhance reliable transmission of electricity. The Lone Star 345 kV transmission network corridor, shown in Fig. 1 and Fig. 2, has been in service since March 2013 to transmit primarily wind-generated electric power from remote west Texas to northeast Texas. The two main Lone Star 345 kV transmission lines are partially parallel on double-circuit towers with 50 percent series compensation. The lines run from West Shackelford, Scurry County, northwest of Abilene, Texas, to Navarro County, just south of the Dallas Fort Worth metropolitan area.
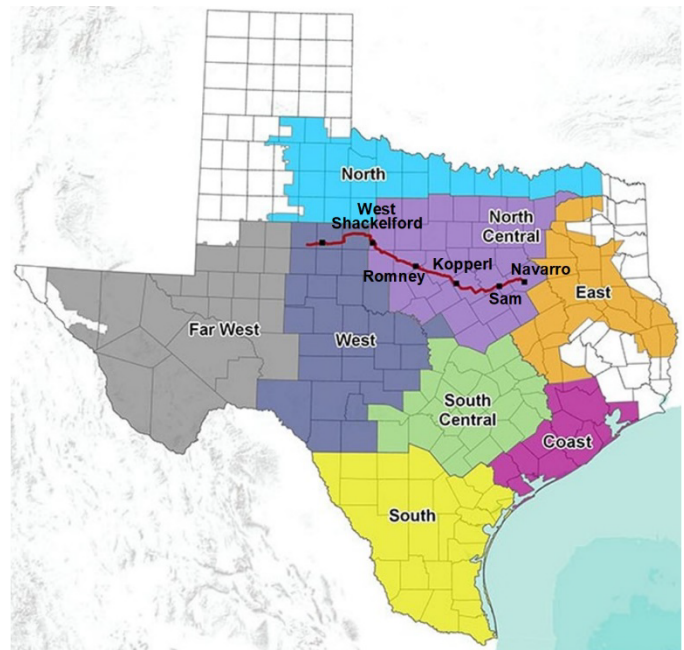
Fig. 1.   Map showing route of 345 kV transmission network corridor.
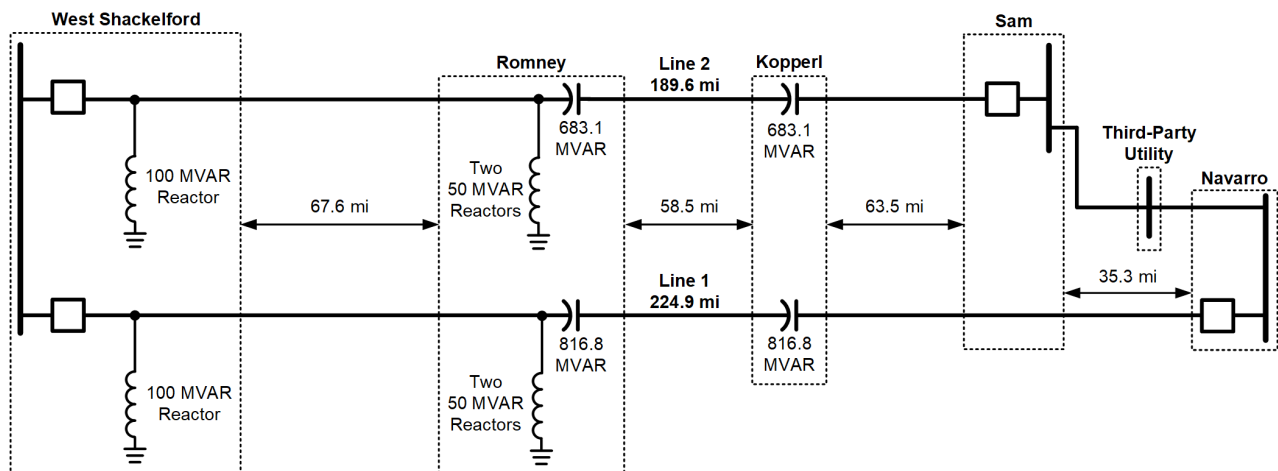
Fig. 2.   Simplified one-line diagram of West Shackelford to Sam (Line 2) and West Shackelford to Navarro (Line 1) series-compensated lines.

At approximately one third and two thirds of the 189.6 mi line (Line 2) are two series capacitor bank substations without fault-clearing circuit breakers, as shown in Fig. 2. These substations are Romney toward the west and Kopperl toward the east. In addition, Romney also has 50 MVAR shunt reactors, two for each line. The West Shackelford terminal has one 100 MVAR shunt reactor on each line (the shunt reactor circuit breakers are not shown). The shunt reactors are applied for reactive power compensation during light load conditions, especially at night, to absorb reactive power and reduce line voltage. These shunt reactors allow for five steps of reactive power compensation, 0, 50, 100, 150, and 200 MVAR. The series capacitor bank bypass switch, isolation switches, metal-oxide varistors (MOVs), bypass circuit breaker, and discharge damping reactor are shown in Fig. 3 and partially in Fig. 4.
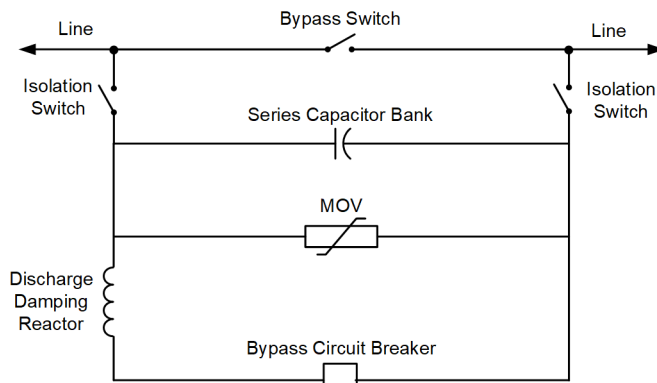
Fig. 3.   Capacitor bank one-line diagram [1].
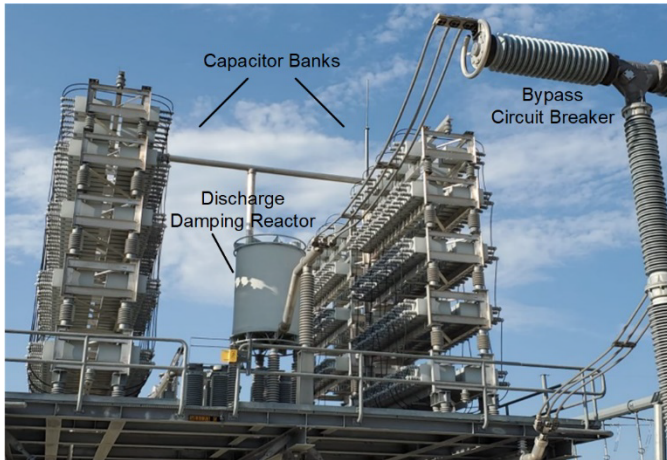
Fig. 4.   Series capacitor bank substation.

As a result of the original system planning studies, Lone Star chose to use high-speed redundant protection schemes for each line. They designed the line such that a trip on the line will initiate a bypass operation to the bypass circuit breaker on both series capacitor banks [2]. The line protection system for Lone Star consists of three levels of protective relaying [2], as shown in Fig. 5.

The first level of protection is line current differential (87L). This level of protection consists of three 87L1 relays in a three-terminal arrangement: one for each line terminal and a third at Romney. The addition of the 87L1 relay at Romney creates a differential protection zone so that shunt reactor faults do not trip the line. This zone is necessary because the reactor has its own protective relays (87R and 51), and the line should only trip as a backup for a reactor fault.

The relays in the second level provide line distance protection (21L) by using a directional comparison blocking (DCB) scheme. The DCB scheme uses dual communication through both a digital multiplexer and power line carrier. One 21L relay is installed at each line terminal. The Zone 1 relay setting at Sam is based on the distance from Sam to Romney. This is to prevent the Zone 1 distance element from overreaching into the reactors at Romney. The series capacitor banks alter the line reactance and may cause the Zone 1 element to overreach. The distance relay has settings that can account for capacitor banks, but they have not proven to be very reliable.

The third level of protection is an additional series of 87L2 relays that divides each line into three segments: West Shackelford to Romney, Romney to Kopperl, and Kopperl to Sam. Each line segment has two 87L2 relays. This second differential protection zone protects the line in case the other levels of relaying fail to trip because of the series capacitor banks. In addition, dividing the line into three segments makes locating the faulted segment easier. The faults that occur between the capacitor bank substations have been the most difficult to locate. It is for this reason that Lone Star made the decision in 2019 to install two ultra-high-speed (UHS) relays with traveling-wave fault-locating (TWFL) capability on both lines.

The four UHS relays at Lone Star, shown in Fig. 6, are for standalone high-resolution digital fault recording, fault locating, and line monitoring. They currently do not trip any circuit breakers.

The UHS relay pilot installation on Line 1 and Line 2 included the underreaching directly tripping TD21 element (incremental quantity Zone 1) and the two-terminal permissive overreaching transfer trip (POTT) scheme. The POTT scheme has been configured to use the TD32 and TW32 directional elements [3].

See Section III of [4] for a summary of the fundamental principles of the TW32, TD21, and TD32 elements for UHS line protection.

A third UHS relay at Romney for Line 1 and Line 2 is needed to improve from a two-terminal to three-terminal POTT scheme arrangement to exclude Romney reactors from the POTT scheme. This requires adding two UHS relays (one per line) and a digital multiplexer at Romney. An added advantage is that reactor faults at Romney become out-of-zone line faults. However, as explained more in Section IV, dividing each line into three segments with two UHS relays per segment is preferred. The segments would be West Shackelford to Romney, Romney to Kopperl, and Kopperl to Navarro or Sam. For an explanation of two-terminal and three-terminal POTT schemes in UHS relays, see [3].
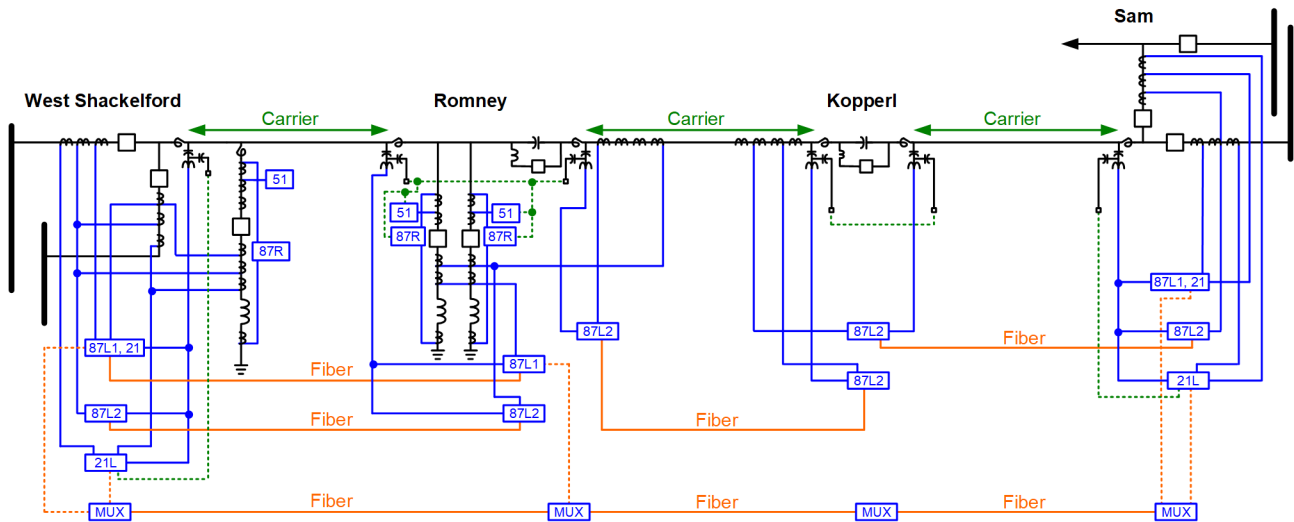
Fig. 5.   West Shackelford to Sam (Line 2) protection one-line diagram [2].
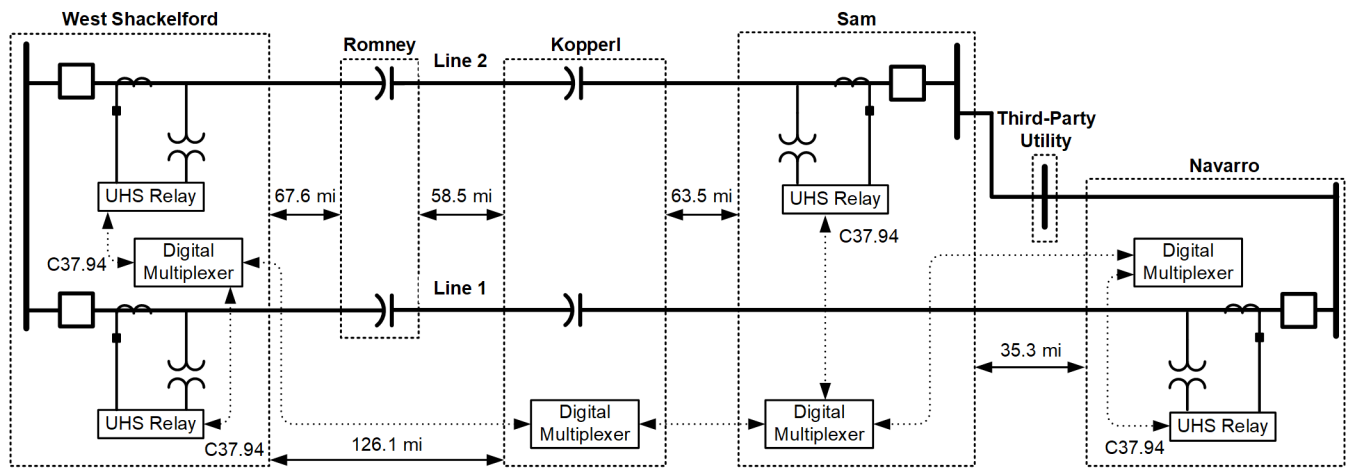
Fig. 6.   Simplified one-line diagram of UHS relays and dedicated C37.94 communications network for West Shackelford to Sam (Line 2) and West Shackelford to Navarro (Line 1).

UHS relays require a different testing method than traditional relay testing methods. Therefore, Lone Star experimented with a system-based testing approach, combining software and hardware, that could generate test signals with realistic transitions and precisely controlled TW pulses. With this approach, we performed a full end-to-end system-based test with the UHS relays installed in their applied environment and location. In addition, we modeled the entire transmission line system in software with both capacitor banks and the reactors on the line to see how the UHS relays would respond with a more realistic model. Lastly, with the relays and their dedicated digital multiplexers installed, we verified the C37.94 channel between the UHS relays, see Fig. 6, and tested the POTT scheme and the double-ended traveling-wave fault-locating (DETWFL) method.

This paper summarizes how we performed the UHS relay on-site testing, provides results of that testing, and documents recent internal faults on both lines. Section II explains the testing model, setup, requirements, and verification recently performed on Line 2. Section III provides the testing objectives, scenarios considered, results obtained, and technology limitations. Section IV discusses improving line protection by

using UHS relays. Section V provides field experience results from the UHS relay event records that confirm performance expectations.

II.   TESTING METHOD

We tested the incremental-quantity distance (TD21) element, the incremental-quantity directional (TD32) element, the TW-based directional (TW32) element, and the two-terminal POTT scheme protection. In addition, we tested the fault locator within the UHS relay for accuracy. Details regarding the fundamental principles and testing of these elements and TWFL are described in [5], [6], [7], and [8].

A.   Testing Model

During the October 2020 scheduled outage of Line 2 (West Shackelford to Sam), we performed on-site testing of the UHS relays with application-specific settings. Testing TW and incremental-quantity elements places specific requirements on the input signals to the relays. Traditional testing methods, which use test signals in a state-based sequence, are not sufficient, and a new testing method had to be used [5] [7] [9].
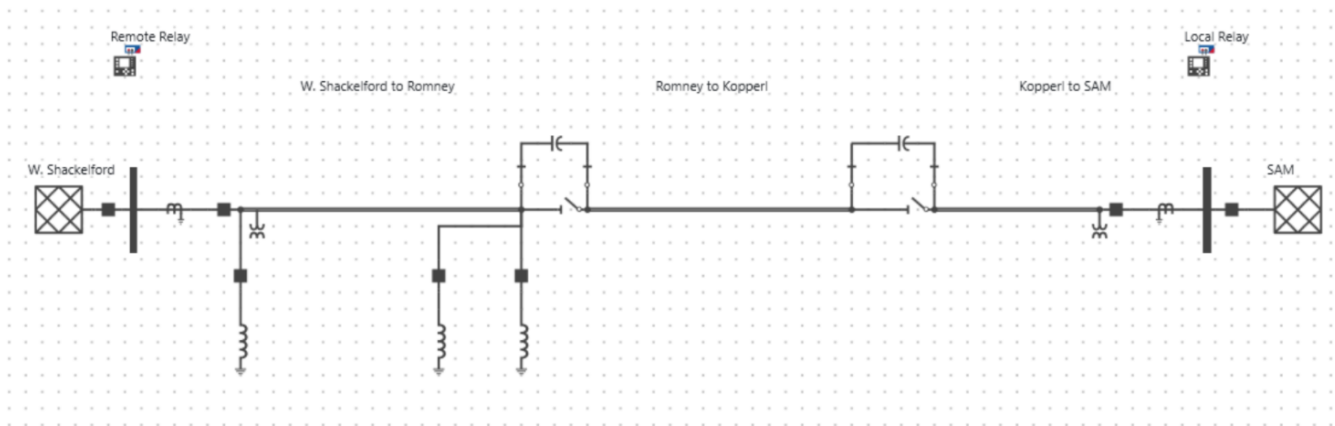
Fig. 7. Topology of Line 2 with capacitor banks and shunt reactors in service.
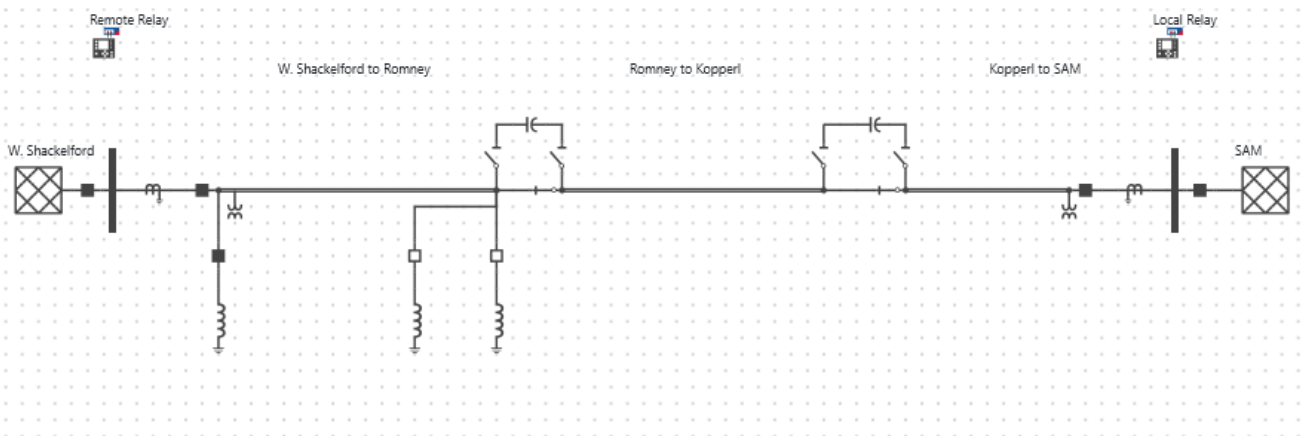
Fig. 8. Topology of Line 2 with capacitor banks and Romney shunt reactors bypassed.

This end-to-end system-based testing method defines a model of the power system in simulation software. Using the software, we drew the topology of the protected line, including infeeds (sources), and entered relevant parameters such as system voltage, short-circuit values, capacitor bank and shunt reactor values, CT polarity, line length, and TW line propagation time (TWLPT).

The simulation software allowed us to simulate various operational conditions such as bypassing capacitor banks and switching shunt reactors in and out of service, as shown in Fig. 7 and Fig. 8.

B. Setup

TW-based elements in the UHS relays can be triggered by using 5 µs rise time current and voltage pulses that have sharp and distinct signal edges. In our case, the TW32 element is used only for keying the POTT scheme and the TD21 and TD32 elements operate on incremental quantities, coupled with the requirement to first enable the arming logic for these protection elements [3] [5]. Hence, realistic current and voltage signals are needed in addition to TW pulses.

To test these elements, the software integrates both the transient simulation signals, including the transition from pre-fault to fault with decaying dc offset, and the TW pulses [5]. Using the setup shown in Fig. 9, we successfully tested all the

applied TW and incremental-quantity-based elements simultaneously.
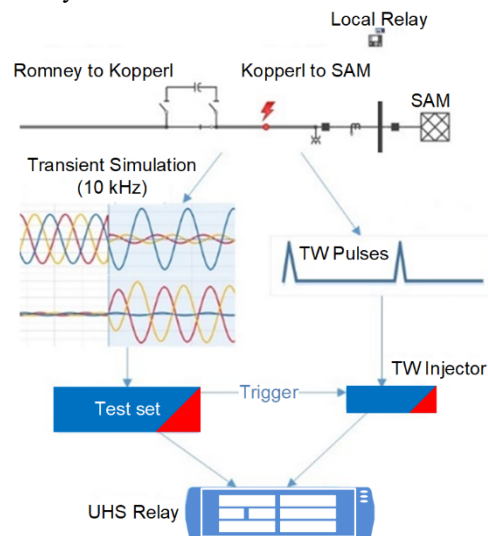
Fig. 9. TW pulses superimposed on conventional test signals [5].

During simulation of an internal fault, a TW injector accessory at each terminal generates the initial voltage and current TW pulses at a time calculated from the system model, TWLPT setting, and selected fault location for the test case. The first TW pulses simulate the first TWs arriving at the terminal

from the fault. Then, the TW injector generates a second set of voltage and current TW pulses, corresponding to the arrival of a second set of TWs. These second TW pulses represent the first TW reflections from the terminal that traveled back to the fault and reflected back to the terminal. The relay uses the arrival time of the second TWs in single-ended traveling-wave fault locating (SETWFL); see Fig. 31.

C. Hardware Requirements

At each line terminal, we connected a conventional test set and a separate TW injector to the respective UHS relay test switches via standard test plugs. We connected the TW injector currents in parallel with the conventional test set currents and connected the voltage signals in series [7]. Fig. 10 shows only the A-phase-to-ground (AG) connection from the TW injector, for clarity of view, but during testing, all three phases were connected. The test set supplies transient simulation signals at a 10 kHz sampling rate, while the TW injector generates TW pulses with a time resolution in the submicrosecond range [5]. Each setup (shown in Fig. 11) is connected to a PC running the simulation test software. At the local terminal, the PC establishes control of the local test set and TW injector. At the remote terminal, a proxy application is run on the PC, and a 4G LTE cloud connection enables the PC at the local terminal to control the remote test set and remote TW injector [7].
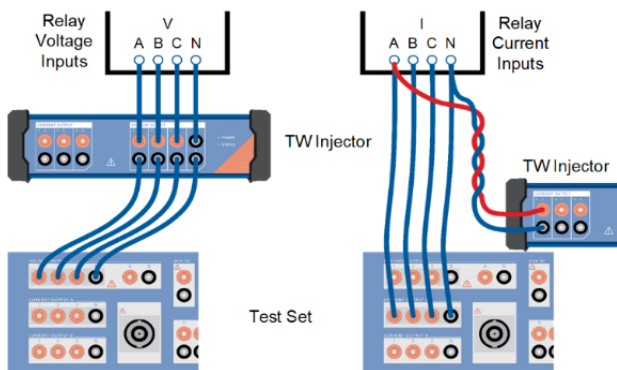
Fig. 10.   Conventional test set and TW injector test wiring for an AG fault.
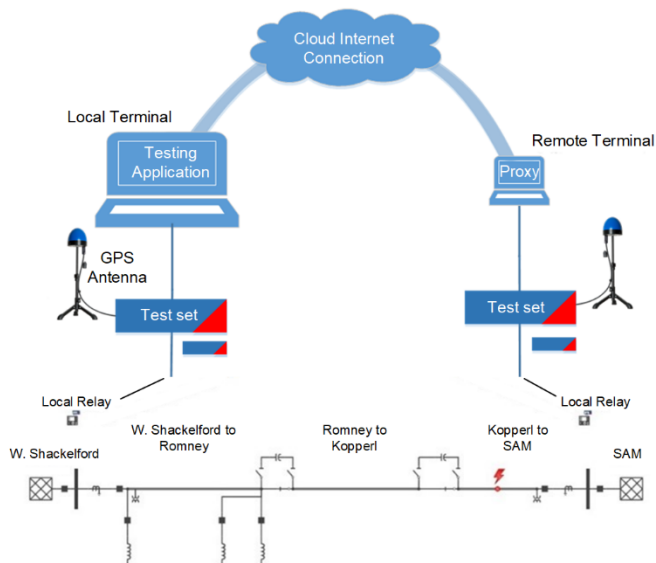
Fig. 11.   End-to-end field test setup [5].

At the local and remote terminals, separate antenna-integrated GPS clocks provide the test sets with time synchronization via IEEE 1588 Precision Time Protocol (PTP).

D. Verification

After installing test equipment and conducting wiring checks, we simulated typical power flow on the line and verified the relay metering. Our verification results are shown in Fig. 12.
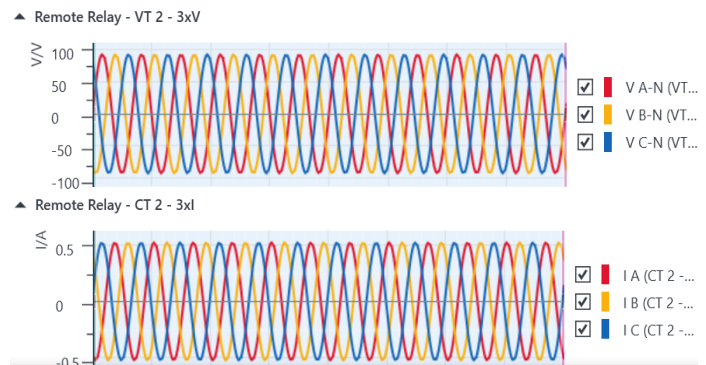
Fig. 12.   Relay metering verification in secondary volts and amperes.

III.   TEST RESULTS

A. Test Goals

As mentioned in Section I, the motivation for Lone Star to install and initially apply the UHS relays was to improve fault-locating accuracy (to within one tower span [1,000 ft or 300 m] on average, regardless of line length), particularly for faults that occur between the capacitor bank substations. To verify this accuracy, we needed a method for testing the impedance-based and TW-based fault-locating performance. Another goal was to efficiently test various operational scenarios, including when the C37.94 channel between the UHS relays was not available.

Fig. 13 shows enabling of the TW pulses in the simulation software, which controls the test set and TW injector.
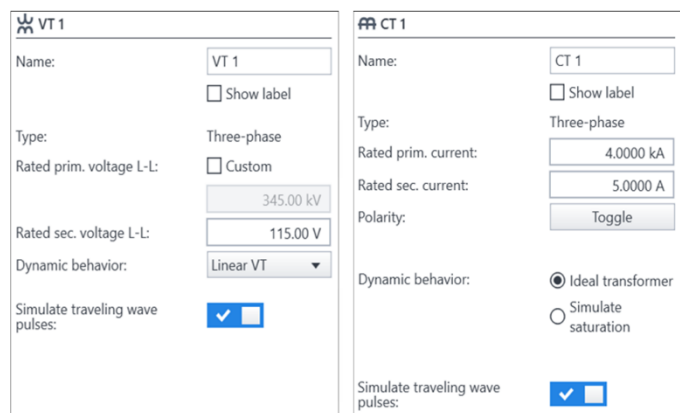
Fig. 13.   Enabling voltage and current TW pulse simulation.

By superimposing TW pulses onto the conventional test set signals, we provided realistic secondary test signals to the UHS relays for concurrent testing of all elements and fault-locating methods under applied conditions. The relay trip outputs are connected to the test set binary inputs to monitor and measure the relay operating times. In this way, we verified the UHS

relay settings, and linked any necessary modifications or adjustments directly to documented testing outcomes.

B. Scenarios and Results

The simulation software also allowed us to easily place faults at different segments along the protected line and to test different fault conditions, such as when either capacitor bank is bypassed or when no TWs are generated. Furthermore, we tested for faults outside the protected zone with the software model. For this testing, it was important to note the polarity and precise timing of the TW pulses and to confirm protection element and scheme security for out-of-zone faults.

For testing purposes, we used 189.07 mi as the entire line length. In the power system model, we divided the line into three segments:

- West Shackelford to Romney: 66.72 mi
- Romney to Kopperl: 58.32 mi
- Kopperl to Sam: 64.03 mi

1) AG Fault at 50 Percent of the Kopperl to Sam Line Segment With Generated TW Pulses

In one test case, after switching the capacitor banks out of service, as shown in Fig. 14, we increased the fast overcurrent supervision in the UHS relays to provide security for the POTT scheme [3].

Fig. 15 shows the DETWFL results from each relay: the relay at West Shackelford declared the fault at 157.536 mi and the relay at Sam declared the fault at 32.064 mi. Considering the line and segment lengths as well as the location where the fault was placed in the model (157.06 mi from West Shackelford and 32.02 mi from Sam), this is a highly accurate result. The accuracy is also confirmed by the Bewley diagram in Fig. 16.

The TD21, TD32, and TW32 elements asserted on the local relay, while the TD32 and TW32 elements asserted only on the remote relay. These are logical results given that the TD21 Zone 1 reach point on each of the relays was set to 70 percent of the total line length.
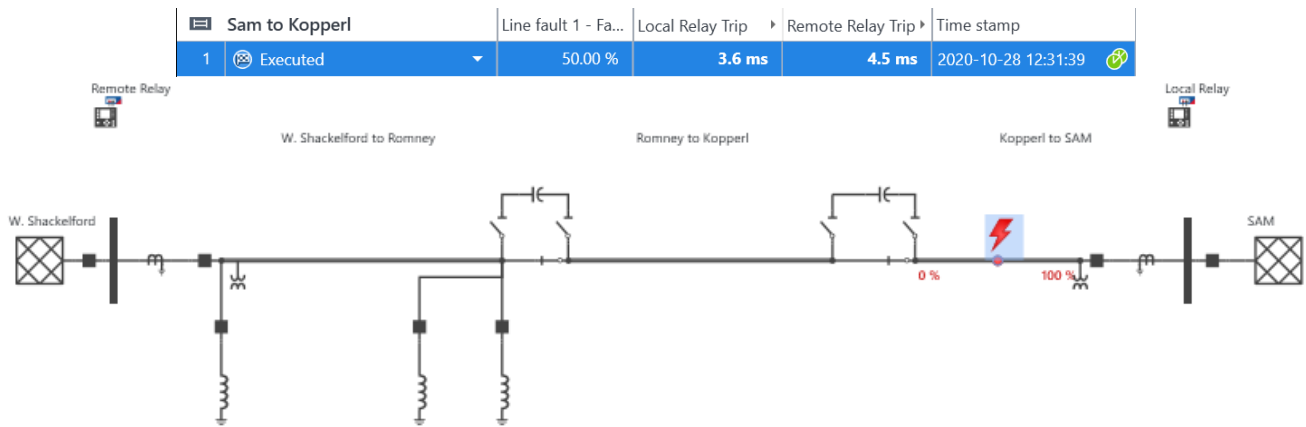
Fig. 14.   Topology for the test case with a fault on the protected line with capacitor banks bypassed.
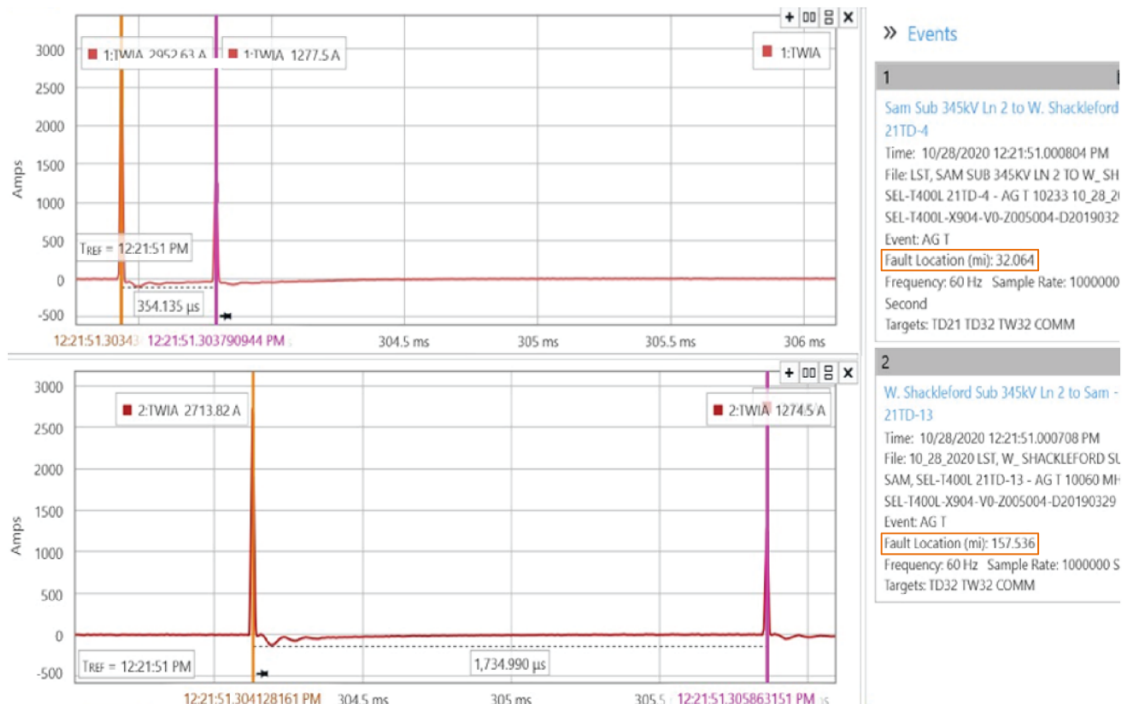
Fig. 15.   UHS relay event showing the TW pulses at Sam (top) and West Shackelford (bottom).
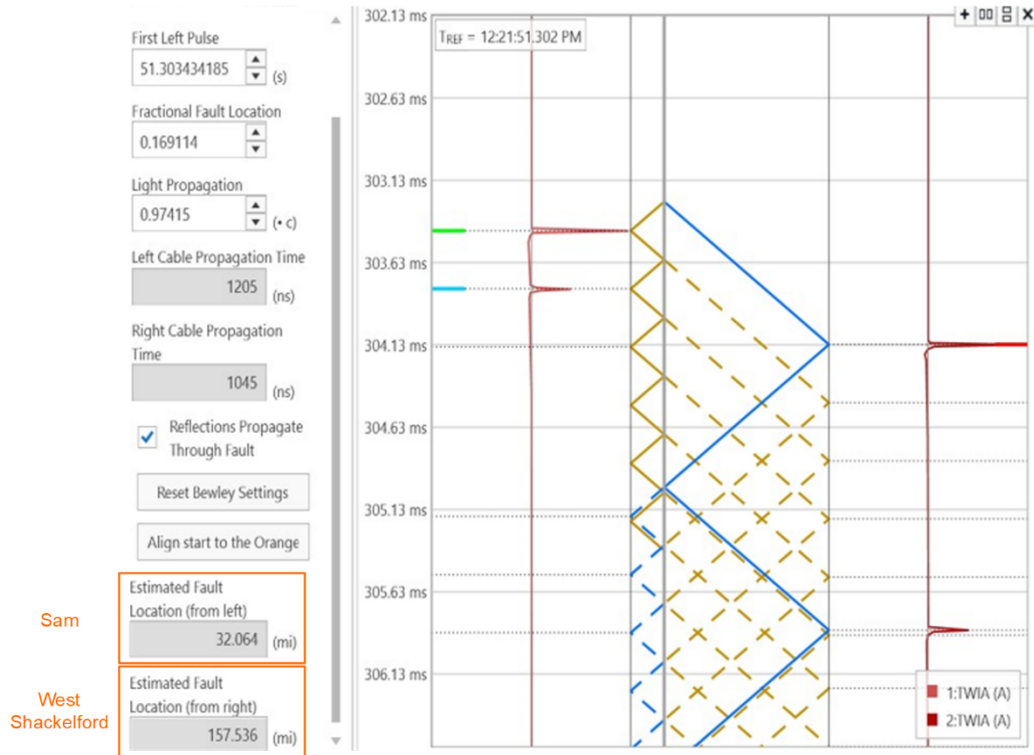
Fig. 16. Bewley diagram generated with relay fault records for the simulated fault in Fig. 15.

2) AG Fault at 50 Percent of the Romney to Kopperl Line Segment With Generated TW Pulses

In the simulation model, with the capacitor banks in service, we placed a fault at the midpoint of the Romney to Kopperl line segment (Fig. 17) that is $66.72 + 58.32 \cdot 0.5 = 95.88$ mi from West Shackelford and $64.03 + 58.32 \cdot 0.5 = 93.19$ mi from Sam.

The relays declared the faults at 96.202 mi from West Shackelford and 93.398 mi from Sam, as shown in Fig. 18. Again, this shows that the DETWFL method is very accurate.

In Fig. 18, the targets show that the TD32 and TW32 elements asserted but the TD21 element did not, even though the fault was approximately in the middle of the line and the Zone 1 reach settings for the UHS relays at each terminal were set to 70 percent. These and other challenges are discussed in Section III. C.
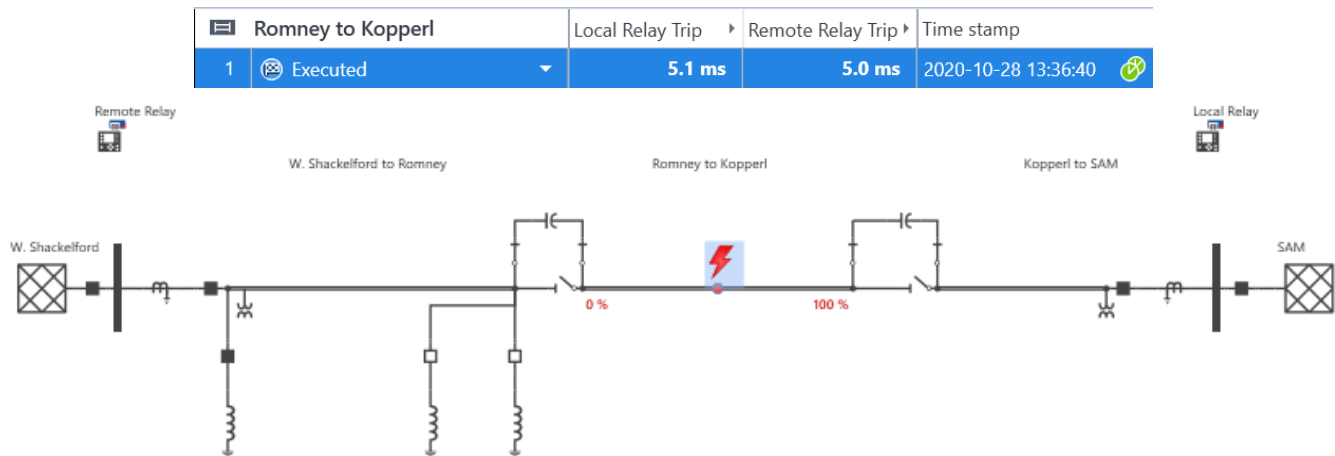
Fig. 17. Topology for the test case with a fault on the protected line with capacitor banks in service.
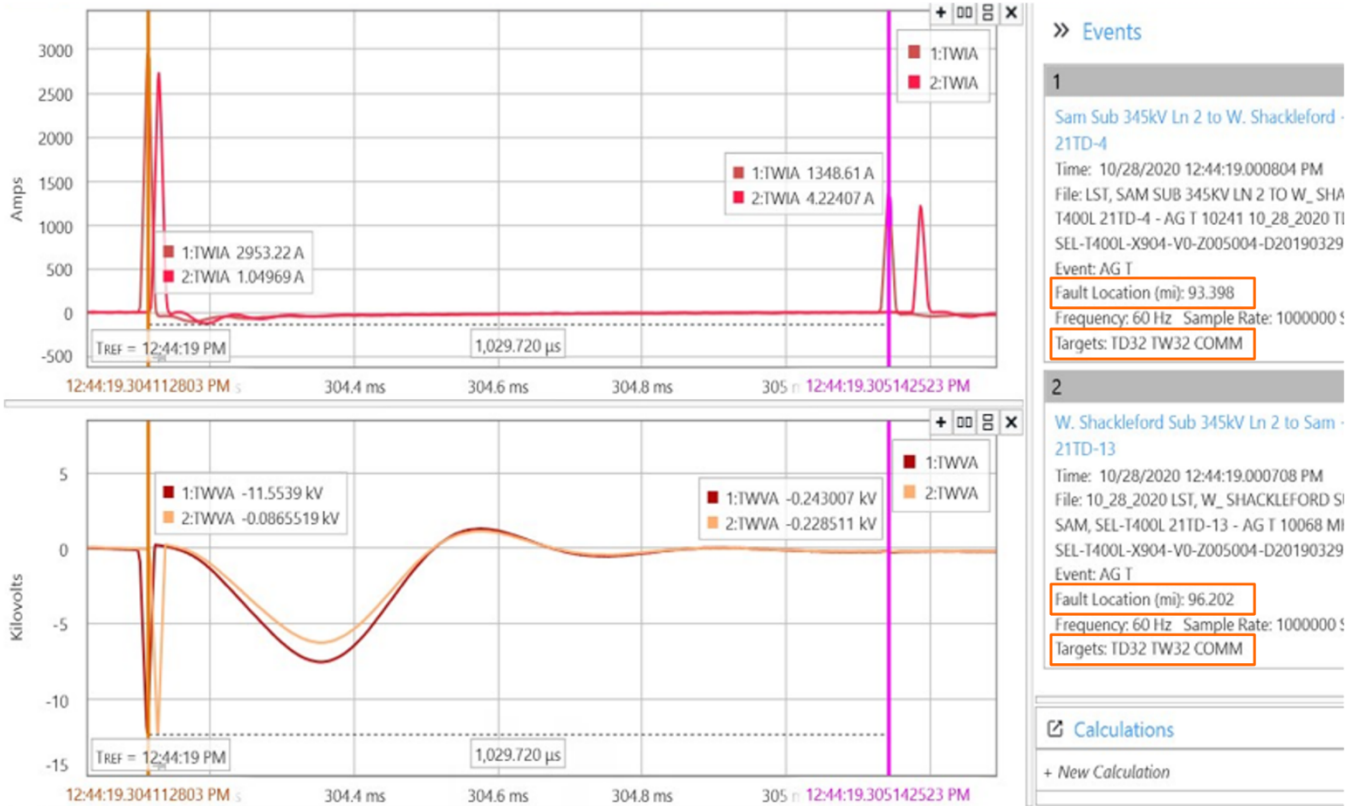
Fig. 18.   UHS relay event records showing current TW pulses and in-phase polarities (top) and voltage TW pulses (bottom) for the simulated fault in Fig. 17.

3) POTT Scheme Disabled

For this simulation, we simulated a fault at the midpoint of the Romney to Kopperl line segment and removed the communications channel, which disabled the POTT scheme. We observed that the TD21 elements underreached and neither of the UHS relays at either terminal tripped, as shown by the $+\infty$ in Fig. 19.

4) AG Fault at 90 Percent of the Romney to Kopperl Line Segment With No Generated TW Pulses

By changing the fault inception angle to zero degrees on the simulation software, we generated no TW pulses, only transient signals with a 10 kHz bandwidth. See Fig. 20.

The UHS relays tripped, local (Sam) in 5.3 ms and the remote (West Shackelford) in 6.7 ms (1.4 ms slower). The fault-locating results were unreliable. Neither UHS relay could reliably locate the fault (error of tens of miles). Without TW pulses, the UHS relays provided only single-ended impedance-based (phasor) fault-locating (ZFL) results (double-ended ZFL is only available over direct fiber communications) [3]. See Fig. 21. Fault-locating dependability was seriously affected for faults between the series capacitors, which was expected. This is further discussed in Section III. C.
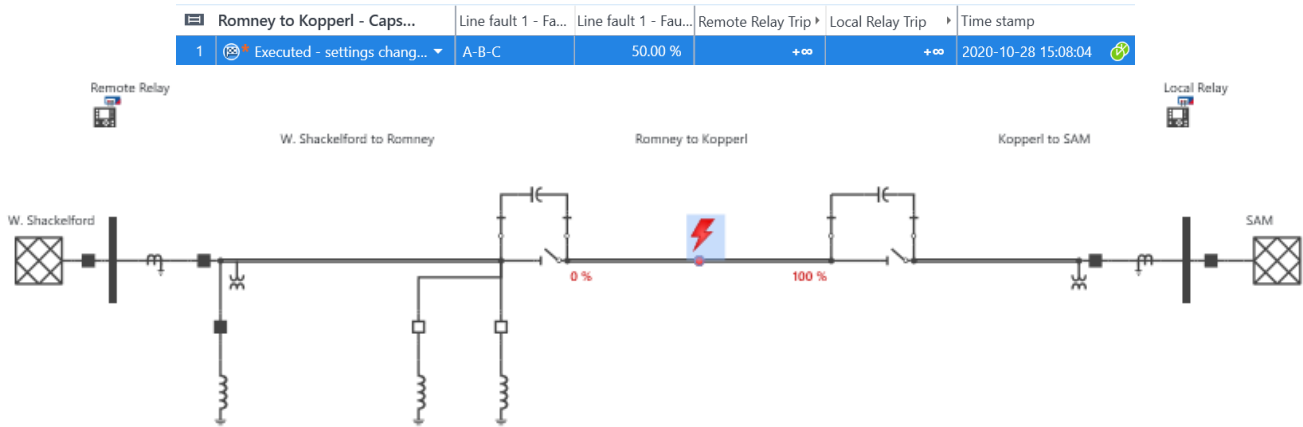
Fig. 19.   UHS relay response with communications channel removed.

No TW - Romney to Kopp...		Line fault 1 - Fa...	Line fault 1 - Fau...	Remote Relay Trip ▸	Local Relay Trip ▸	Time stamp
1	⊗ Executed ▾	90.00 %	A-N	6.7 ms	5.3 ms	2020-10-28 16:50:29

Remote Relay

Local Relay

W. Shackelford to Romney

Romney to Kopperl

Kopperl to SAM

W. Shackelford

SAM

0 %   100 %
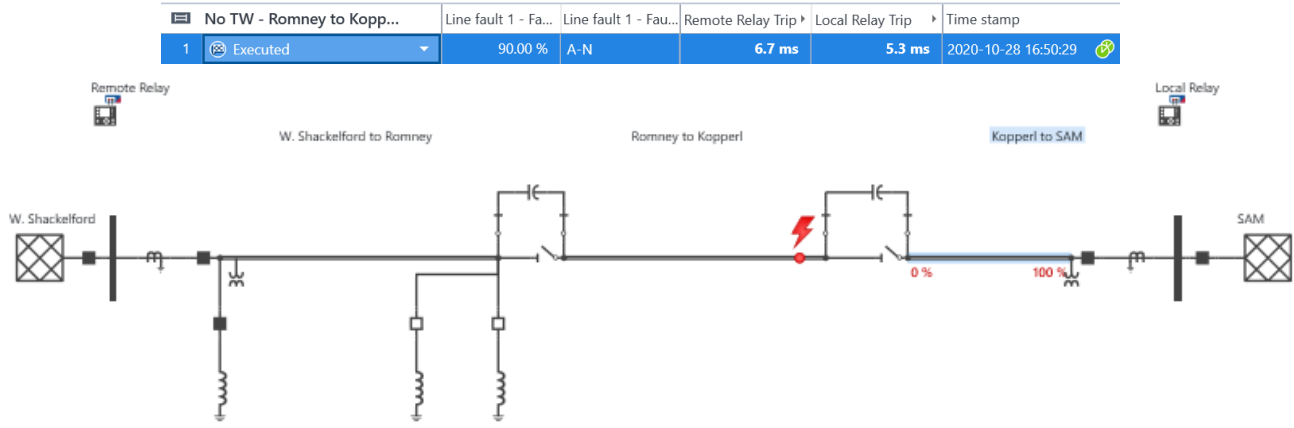
Fig. 20.   Topology for the test case with a fault on the protected line and no TW pulses.
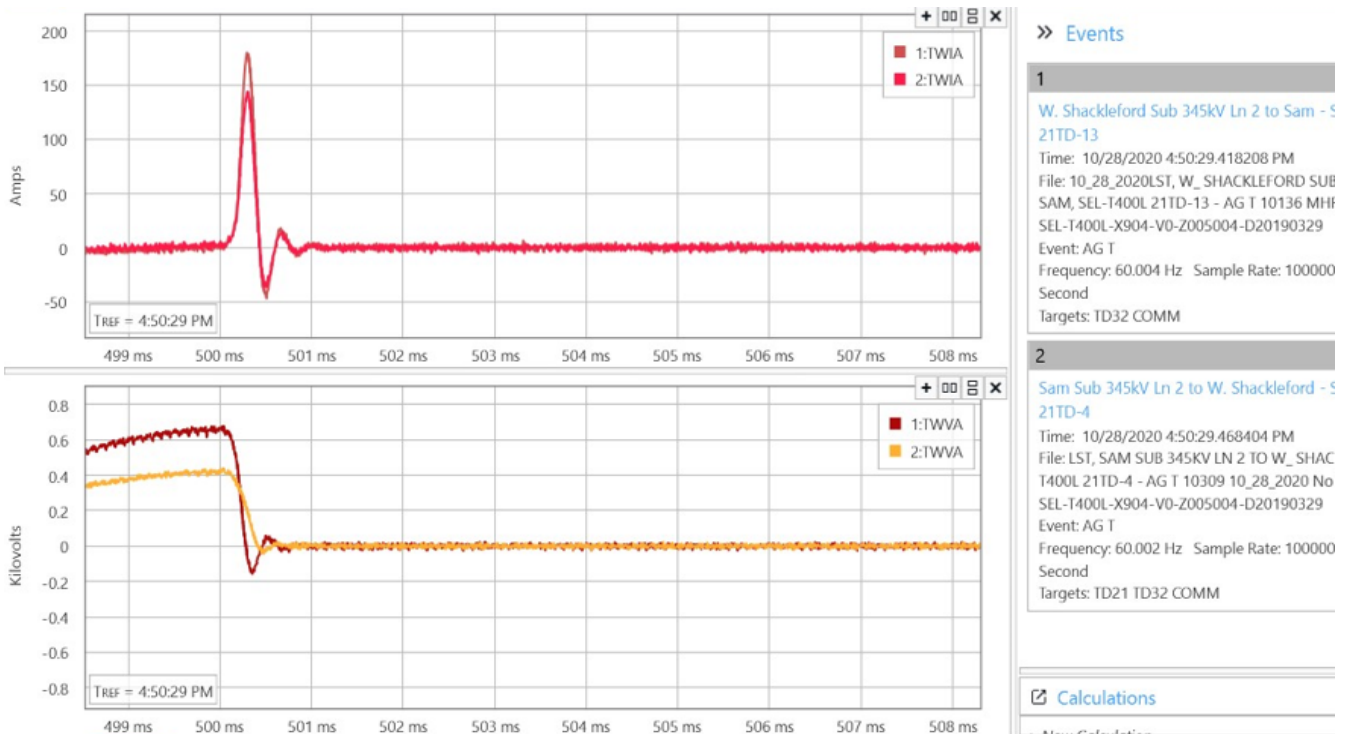
Fig. 21.   UHS relay event records showing test set signals only, no TW pulses.

Fault on Local Busbar		Node fault 1 - F...	Local Relay Trip ▸	Remote Relay Trip ▸	Time stamp
1	⊗ Executed ▾	A-N	+∞	+∞	2020-10-28 16:15:54

Remote Relay

Local Relay

W. Shackelford to Romney

Romney to Kopperl

Kopperl to SAM

W. Shackelford

SAM
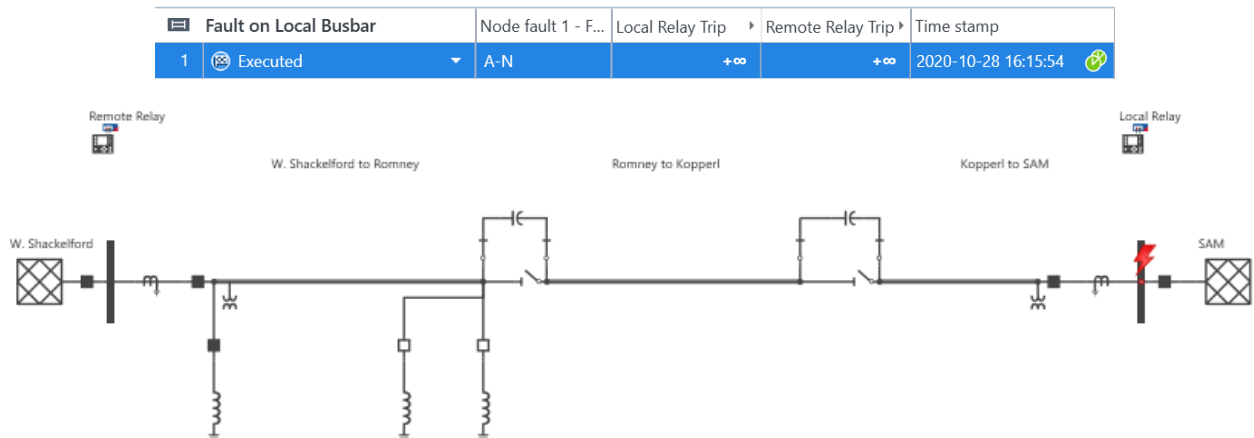
Fig. 22.   Fault on the bus behind the relaying CT and VT on Sam (local terminal).

5) AG Fault External to the Protected Line

For an external fault, the UHS relays on both terminals restrained from operating, confirming the security of the protection elements and scheme. See Fig. 22.

C. Limitations

As with any technology, the UHS relay TW-based and incremental-quantity-based elements have dependability limitations, such as 1) faults that launch small TWs (point-on-wave challenge), 2) faults that are very close to a line terminal (TWs frequently reflect and overlap), and 3) the underreaching behavior of the TD21 element for weak-infeed conditions (SIR > 2.5) [10].

In addition, series compensation also introduces line protection challenges. Series capacitors dramatically impact distance elements and impedance-based fault locators. This is discussed in detail in [2].

For faults where TWs are not launched or detected, the UHS relays default from TWFL methods to ZFL methods. The main limitation on lines with series capacitors is the nonlinear resistive-capacitive impedance of the series capacitors with MOVs (see Fig. 5). Neither ZFL method (single-ended or double-ended) is suitable for series-compensated lines unless specifically designed to cope with series-compensation [6]. Typically, the fault appears closer than it really is because of the negative reactance of the series capacitors.

IV. LINE PROTECTION IMPROVEMENTS

A. Zone 1 Setting Improvement

During testing, we observed that the UHS relays underreached for faults between the capacitor banks. The Zone 1 impedance reach of the UHS relay can be set between 0.1 pu and 0.9 pu of the line impedance. Originally, the UHS relays were set to 0.7 pu for a conservative approach to prevent the relay from overreaching. For faults placed at 50 percent of the line length on the Romney to Kopperl line segment, the TD21 element did not pick up for either relay, as explained in Section III. B. 2) and shown in Fig. 18.

The same results occurred when a fault was placed at 10 percent of the line length as measured from Romney on the Romney to Kopperl line segment. We therefore increased the phase and ground reach settings to 90 percent in the UHS relays on both lines during the monitoring phase.

B. Excluding the Reactors From the Line Zone of Protection

On April 14, 2021, a fault occurred on the West Shackelford to Sam transmission line (Line 2). The UHS relay at West Shackelford operated for this C-phase-to-ground (CG) fault (see Section V. A.). The cause of this fault was a damaged bushing on the C-phase of the reactor; see Fig. 23 and Fig. 24. Although one of the UHS relays operated and returned the correct fault location, this was an undesired operation. The reactors have their own set of protective relays that should trip and clear any faults occurring on the reactor. The line protection should only trip as a backup if the reactor fault is not cleared by tripping the reactor circuit breaker. This can be resolved by adding UHS relays to exclude the reactor from the UHS relay zone of protection.

Fig. 23. Damaged reactor bushing at Romney.

Fig. 24. Removed damaged reactor bushing at Romney.

C. Using TW87 Protection

Currently, Lone Star is using the two-terminal POTT scheme and TD21 elements in the UHS relay for protection monitoring (not fault clearing). The TW87 scheme could provide another UHS line protection scheme. The TW87 scheme requires a direct fiber (or wavelength-division multiplexing) channel between the UHS relays for a two-terminal application. Because of the long line length, direct fiber communications is not feasible without optical amplifiers or additional repeater equipment. Currently installed is C37.94 communications for the POTT scheme, DETWFL, and line monitoring. The current plan is to install more UHS relays on

shorter line segments and lines in the system where direct fiber communications is feasible.

Dependable and secure TW87 scheme performance, as shown in [4], [7], [11], and [12], confirmed to Lone Star that TW87, with 1 ms to 3 ms operating time (based on line length), will be valuable in addition to the POTT scheme. Furthermore, adding direct fiber communications for TW87 adds relay-to-relay communications channel redundancy (by using Ports 1 and 6 of each UHS relay) and UHS relay protection redundancy. The channel redundancy in turn provides two, two-terminal POTT scheme keying channels (permissive trip signals), with the direct fiber channel having less latency than the C37.94 channel. The channel redundancy also adds the double-ended impedance-based fault-locating (DEZFL) method. The benefit of faster POTT scheme keying with TW32 is better realized over the direct fiber channel.

D. Upgrading UHS Relays to the Next Model

The UHS relays [3] have been installed to evaluate their protection elements (monitoring and nontripping) and schemes and to provide fault locating (operational). Although secure, as stated in this paper, the protection elements and schemes have dependability limitations. Therefore, they must be paired with phasor-based microprocessor relays that provide line distance and other elements for complete line protection or a UHS relay [10] that includes complete primary and backup line protection.

Lone Star plans to use the line monitoring function in [10] for continuous monitoring of the line by using TWs. The line monitor locates and alarms for non-fault low-energy disturbances and recurring faults on the line, providing specific disturbance locations for patrol crews [13]; see the example in Fig. 59. This technology improves line preventive maintenance and may reduce the number of line faults and unscheduled outages. Lone Star has already observed that the line monitor detects and locates non-fault conductor galloping events that occur during winter storms with high winds and heavy precipitation.

V. FIELD EXPERIENCE

As stated in Section I, the UHS relay pilot installation included the underreaching directly tripping TD21 element (incremental quantity Zone 1) and the two-terminal POTT scheme. The POTT scheme has been configured to use the TD32 and TW32 directional elements [3]. This section uses methods described in [10] and [14] to summarize the observed protection, TWFL, and line monitoring performance for three recent internal faults on the West Shackelford transmission lines: the first on Line 2 and the other two on Line 1.

A. Internal CG Fault on April 14, 2021

On April 14, 2021, a CG fault was recorded by the UHS relays monitoring the West Shackelford to Sam 345 kV 189.6 mi transmission line (Line 2). At the time of the fault, 1) the POTT scheme was not operational because the C37.94 channel was not available (ROKP1 in Fig. 25 deasserted) and 2) the UHS relay at Sam was not GPS time-synchronized.

1) Relay Operating Time

Shown in Fig. 25, at West Shackelford, TD21G asserted in 3.7 ms and TD32F asserted in 2.0 ms. For this fault, TW32F did not assert because of the small initial current and voltage TWs observed at both relays, TWIC was approximately 110 A to 120 A primary, and TWVC was 5 kV primary, as shown in Fig. 26.
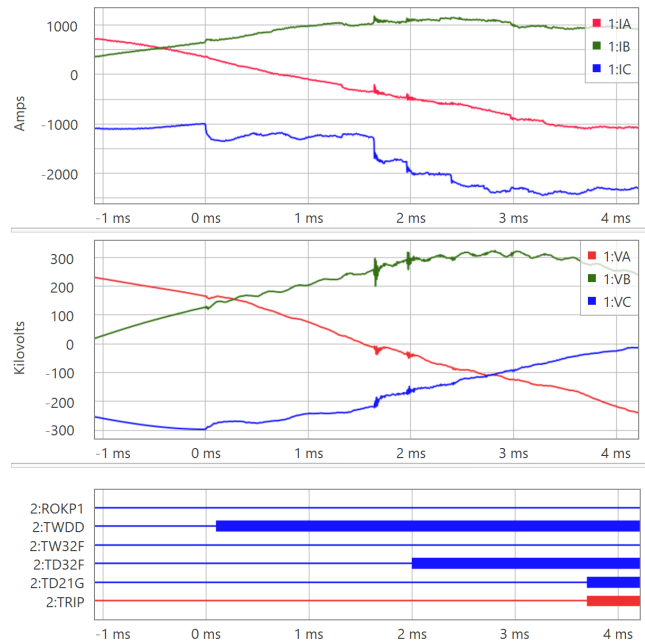
Fig. 25. West Shackelford currents and voltages and digital bits operating times.

Fig. 26 also shows the digital bits related to TW32 and TWDD for both terminals.
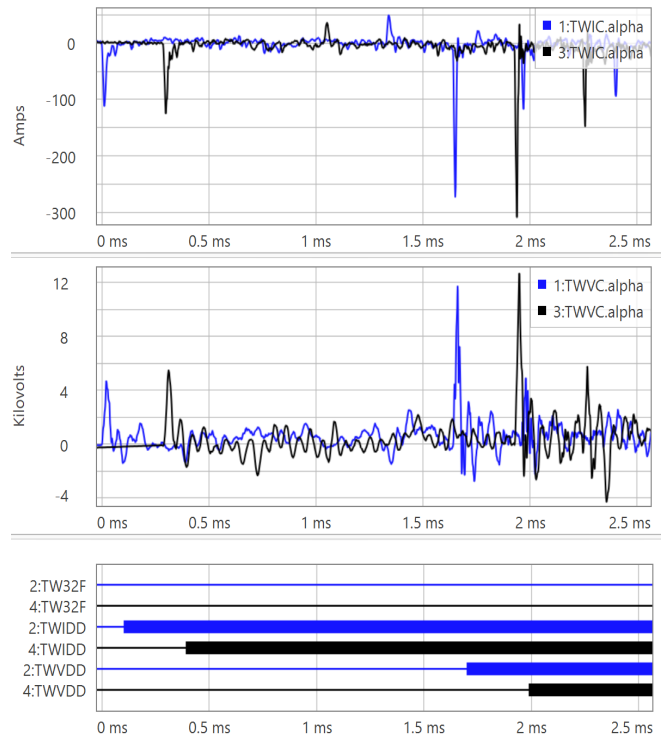
Fig. 26. West Shackelford (blue) and Sam (black) C-phase alpha-mode current and voltage TWs and digital bits operating times.

From Fig. 26, we observe the assertion of both TWIDD and TWVDD (the current and voltage TW disturbance detectors, respectively) in UHS relay logic TWDD = TWIDD OR TWVDD [3]. Note that TW32F does not assert. The TW32 logic operates only during an initial 50 µs window if the TW torque signal is above a threshold and both TWIDD and TWVDD are asserted. After this window, the TW32 logic is disabled to prevent it from responding to TW reflections and non-fault inception TWs [3].

2) TD21 Element Performance

With a reach of 90 percent, TD21CG asserted at West Shackelford and declared an internal CG fault. The fault was located at 36.1 percent (68.52/189.60 pu) of the line length, well within the reach of the TD21 underreaching Zone 1 element. TD21CG operated in 3.7 ms, as shown in Fig. 27. As measured from Sam, the fault was located at 63.9 percent (1 – 0.361 pu) of the line length, which is within the 90 percent reach of the TD21 element. However, TD21CG did not assert. This is because, as shown in Fig. 28, the calculated voltage operating signal (VOP), which is the change in the voltage at the reach point, remained below the calculated voltage restraining signal (VRT). VRT is the pre-fault voltage at the reach point. The TD21 operating window expired 6 ms after the logic detected a CG fault (FSCG). The TD21 operating window is shortened for series-compensated lines to improve security. The TD21 element restrained because of the point on wave when the fault occurred. Had the fault initiated under the same system conditions at a more favorable point on wave, the TD21 element would likely have operated. The farther the fault is from the UHS relay, the weaker the system, the higher the fault resistance, and the narrower the point-on-wave angle for which the element operates [8].
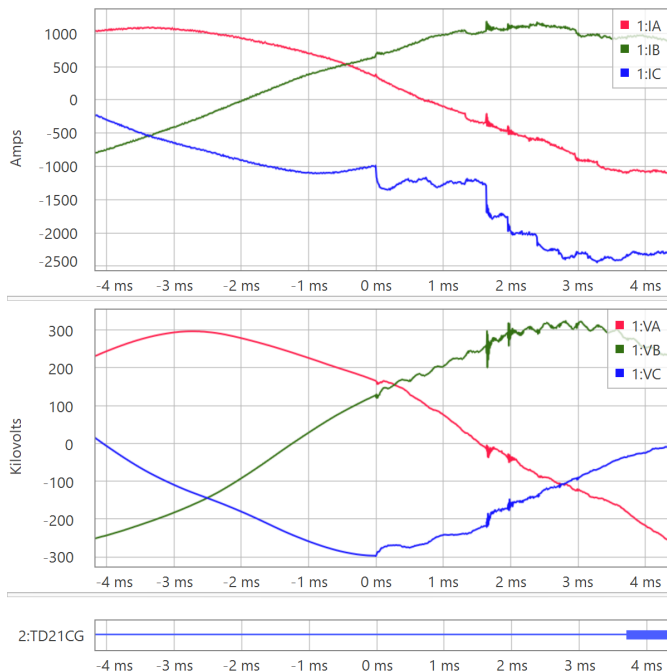
Fig. 27.   West Shackelford TD21CG operated in 3.7 ms.
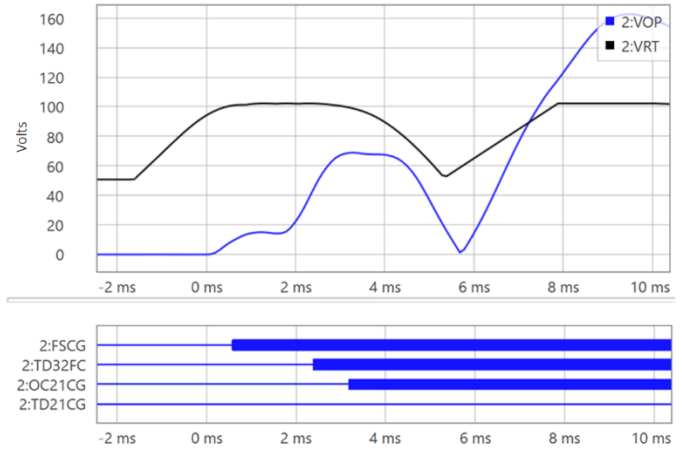
Fig. 28.   Sam TD21CG restrains.

3) POTT Scheme Performance

TD32F operated and detected the fault as a forward fault in both relays. TD32F asserted in 2.0 ms at West Shackelford, shown in Fig. 29, and in 2.4 ms at Sam, shown in Fig. 30. Fig. 29 and Fig. 30 show that incremental quantity replica loop current is opposite in polarity to the incremental quantity loop voltage (see [3] for an explanation of loop voltages and loop replica currents). The incremental quantity replica current for the CG loop can be calculated by using event analysis software (DIZCG = DIZC – DIZ0, [3]). The POTT channel has a typical latency of up to 4.2 ms (based on the longer Line 1). If the channel were operational, the POTT scheme would have operated in less than 6 ms.
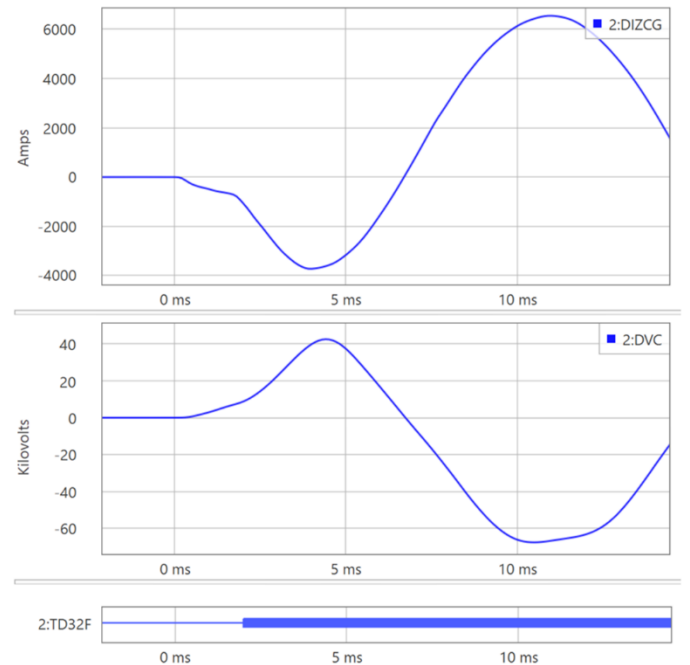
Fig. 29.   West Shackelford TD32F operated in 2.0 ms.
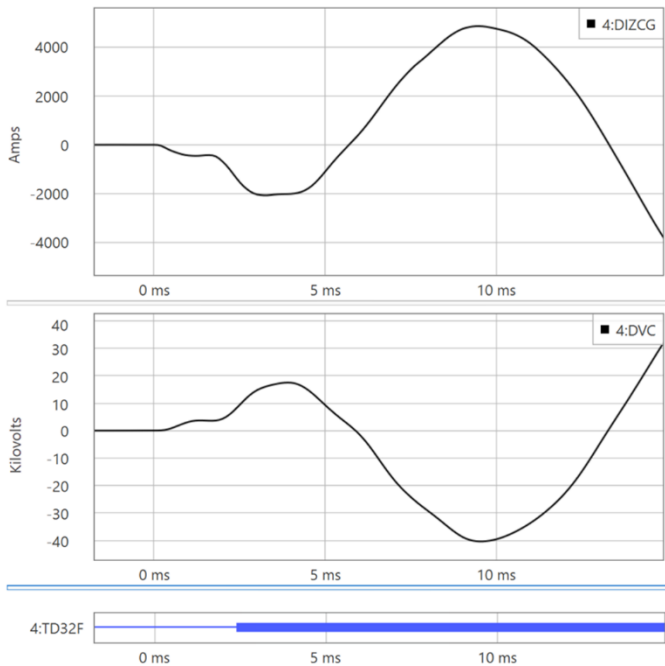
Fig. 30. Sam TD32F operated in 2.4 ms.

4) TW-Based Fault Locating

For this fault, the SETWFL result from West Shackelford was unreliable; therefore, the relay reported the impedance-based method (SEZFL) result of 62.668 mi. Without the C37.94 channel at the time of the fault, DETWFL was not available. Additionally, the UHS relay at Sam was not GPS time-synchronized to allow for calculating DETWFL manually.

We were able to use the SETWFL method by using the West Shackelford SEZFL result as an initial approximation for the fault location. Using this approximation and the larger TWs (second pair of in-phase TWs with magnitudes above 250 A primary) that arrived between 1.5 ms and 2.0 ms in Fig. 26, we determined the time stamps at both terminals, t_1 and t_4, in Fig. 31 [3].
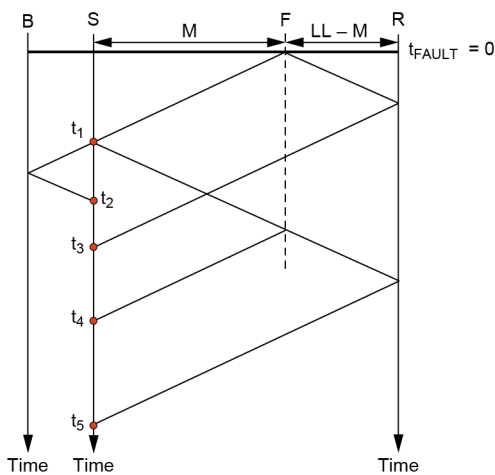
Fig. 31. Bewley diagram explaining the SETWFL method [3].

Fig. 32 and Fig. 33 show the West Shackelford and Sam time stamps t_1 and t_4, respectively, observed and measured with the aid of event analysis software.

Fig. 32. West Shackelford C-phase alpha-mode current TW arrival times: $t_1 = 2.704056189$ s and $t_4 = 2.704806491$ s.

Fig. 33. Sam C-phase alpha-mode current TW arrival times: $t_1 = 2.662918681$ s and $t_4 = 2.664244441$ s.

Using the SETWFL equation (1) from [3],

$$M = \frac{LL}{2}\left(\frac{t_4 - t_1}{TWLPT}\right) \tag{1}$$

where line length (LL) = 189.6 mi and TWLPT = 1044.82 μs, the SETWFL result from West Shackelford is:

$$M = \frac{189.6}{2}\left(\frac{750.302}{1044.82}\right)$$
$$M = 68.077 \ mi \tag{2}$$

and the SETWFL result from Sam is:

$$M = \frac{189.6}{2}\left(\frac{1325.760}{1044.82}\right)$$
$$M = 120.291 \ mi \tag{3}$$

Adding the results from (2) and (3) should equal LL, but 68.077 + 120.291 = 188.368 mi, which is an error of 1.232 mi.

However, we also observe, by definition, that the measured TWLPT from this fault is equal to half of the sum of the two time intervals $(t_4 - t_1)$ from (2) and (3) for a TW that traveled a distance of ½ (2 • M + 2 • (LL – M)), which is LL. So, by using the Bewley diagram shown in Fig. 34, the measured TWLPT = ½ (750.302 + 1325.760) = 1038.03 μs, which differs from the TWLPT setting by 6.79 μs. Also note that TWLPT = ½ $(t_5 - t_1)$.

Substituting the revised TWLPT into (2) and (3), the revised West Shackelford result is:

$$M = \frac{189.6}{2}\left(\frac{750.302}{1038.03}\right)$$
$$M = 68.523 \ mi \tag{4}$$

The revised Sam result is:

$$M = \frac{189.6}{2}\left(\frac{1325.760}{1038.03}\right)$$
$$M = 121.077 \ mi \tag{5}$$
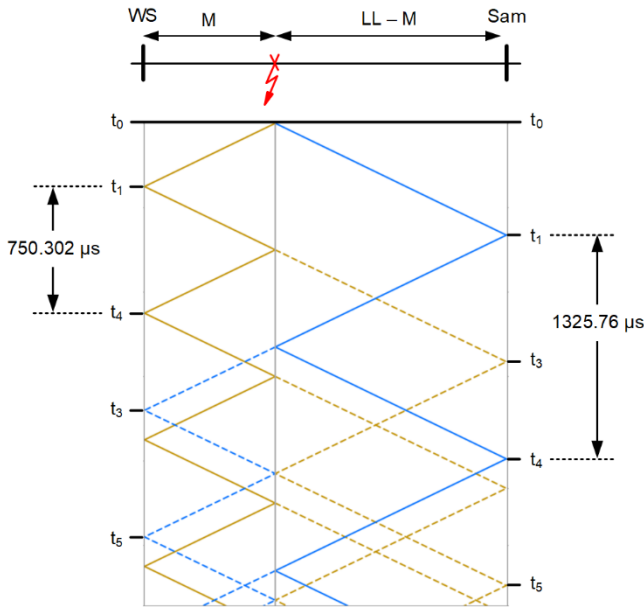
Fig. 34. Bewley diagram for revising TWLPT.

After revising the TWLPT setting, adding (4) and (5) equals LL, 68.523 + 121.077 = 189.6 mi. This fault was caused by a reactor fault at Romney, and the observed fault location was 67.6 mi from West Shackelford and 122.0 mi from Sam. The error of approximately 0.9 mi might be reduced by refining the LL and TWLPT settings with data from future internal and external fault event records.
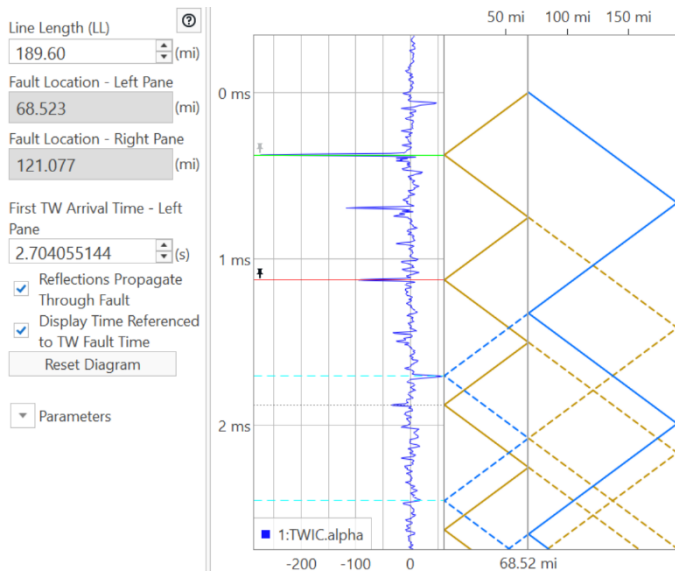
Fig. 35. Bewley diagram showing TW and reflection times at West Shackelford.

The Bewley diagrams in Fig. 35 and Fig. 36 show the time and distance relationship of the measured C-phase alpha-mode current TWs for West Shackelford and Sam, respectively. Each figure has the revised TWLPT setting and shows the first TW (t_1) that arrived at the terminal along with subsequent reflections. Part of the first TW reflects, travels back toward the fault, reflects back from the fault, and then returns to the terminal at t_4 [3]. In these two diagrams, the green time cursor is at t_1, the red time cursor is at t_4, and the cyan cursor is at t_3.

Time stamp t_3 is from the first TW that arrived at the remote terminal. It reflects from the remote bus and returns to the terminal, propagating through the fault and arriving at t_3.
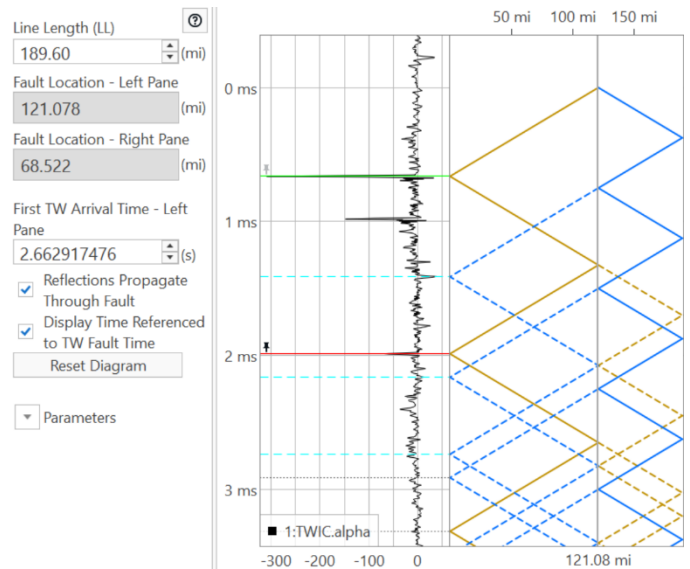
Fig. 36. Bewley diagram showing TW and reflection times at Sam.

B. Internal AG Fault at 17:39:44 UTC on May 11, 2021

On May 11, 2021, an AG fault was recorded by the UHS relays monitoring the West Shackelford to Navarro 345 kV 224.9 mi transmission line (Line 1).

1) Relay Operating Time

Shown in Fig. 37, at West Shackelford, TD21AG asserted in 1.54 ms, TW32F asserted in 0.14 ms, TD32F asserted in 1.04 ms, and the POTT scheme asserted in 5.34 ms.
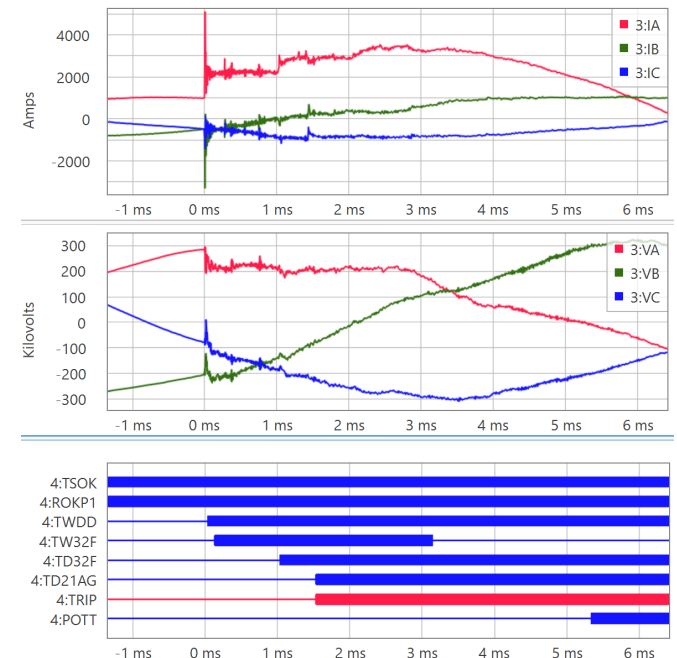
Fig. 37. West Shackelford currents and voltages and digital bits operating times.

Shown in Fig. 38, at Navarro, TD21AG asserted in 2.22 ms, TW32F asserted in 0.12 ms, TD32F asserted in 1.02 ms, and the POTT scheme asserted in 4.82 ms.
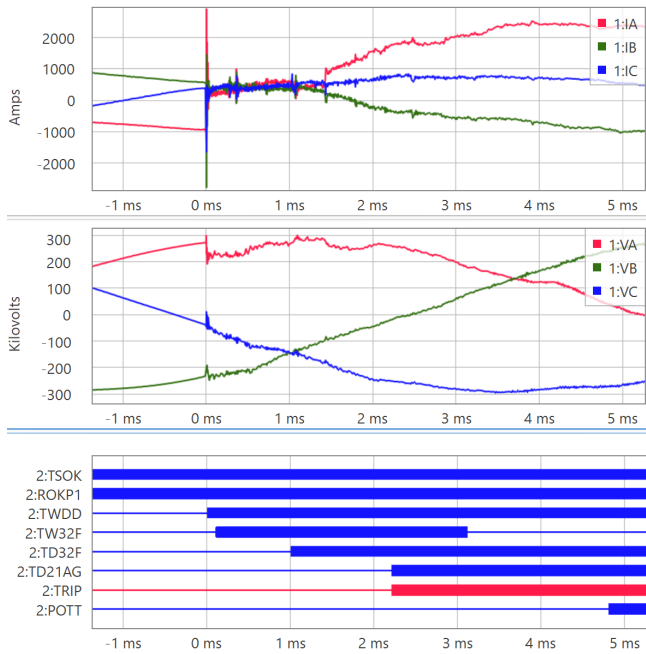
Fig. 38.   Navarro currents and voltages and digital bits operating times.

2)   TD21 Element Performance

With a reach of 90 percent, TD21AG asserted at both West Shackelford and Navarro and declared a Zone 1 AG fault. The fault was located at 41.8 percent (94.03/224.90 pu) of the line length as measured from West Shackelford, well within the TD21 underreaching Zone 1 element reach. TD21AG operated in 1.54 ms, as shown in Fig. 39. From Navarro, the fault was located at 58.2 percent ($1 - 0.418$ pu) of the line length, also within the 90 percent reach of the TD21 element. TD21AG operated in 2.22 ms, as shown in Fig. 40.
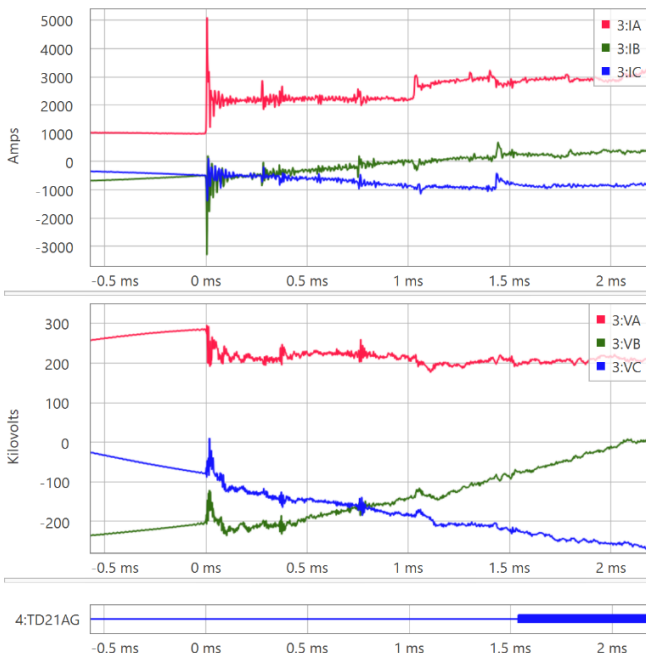
Fig. 39.   West Shackelford currents and voltages and TD21AG operating time.
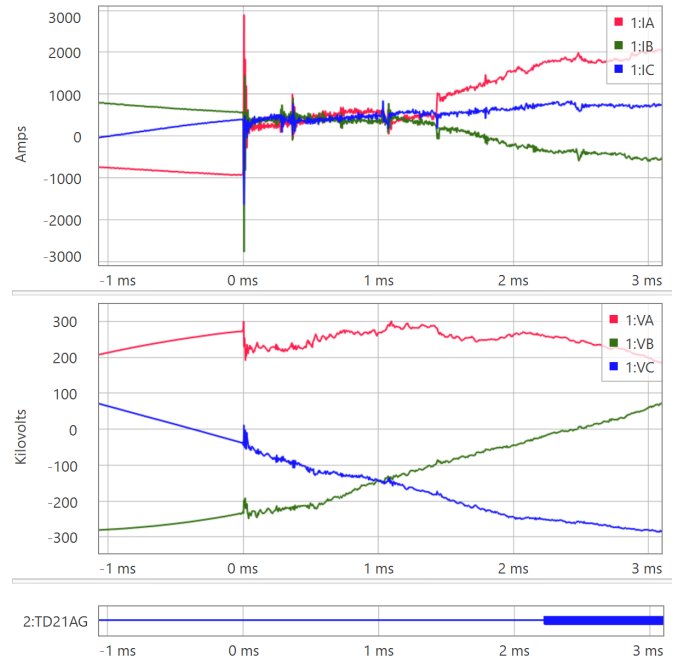
Fig. 40.   Navarro currents and voltages and TD21AG operating time.

3)   POTT Scheme Performance

The UHS relay [3] POTT scheme uses the very fast TW32 and the fast TD32 directional elements and was implemented by using a low-latency C37.94 encoding multiplexed 64 kbps digital channel. With the faster direct fiber channel, the scheme is expected to operate in 1.5 to 6 ms, depending on the fault location and line length [3]. This operating time includes the processing times of both relays of the scheme and the channel latency.
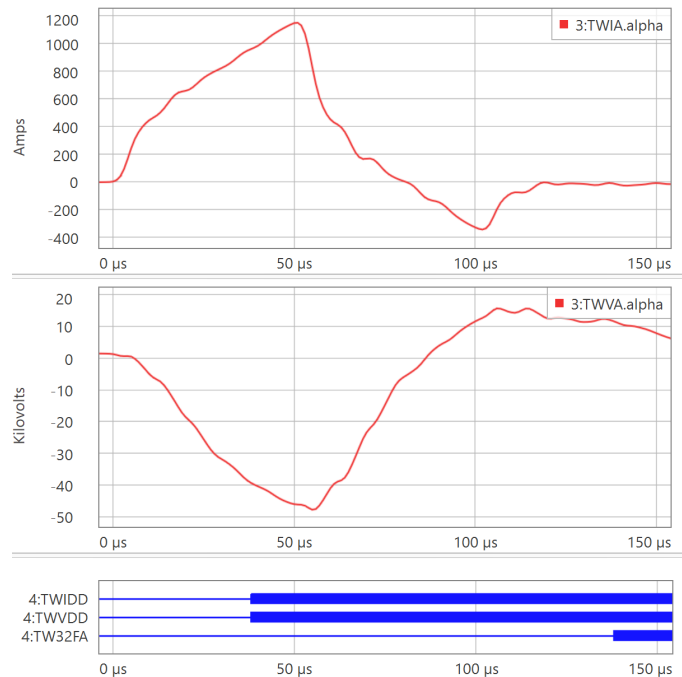
Fig. 41.   West Shackelford A-phase alpha-mode current and voltage TWs and digital bits operating times.

The voltage TW measurement is not accurate in terms of voltage TW magnitude, but it is accurate in terms of the arrival

time and polarity of the first TW, which is sufficient for reliable TW32 element operation.

With CCVTs at both line terminals, we observed that TW32FA asserted and declared a forward fault in less than 150 µs at West Shackelford and Navarro. Opposite polarities of TW currents and TW voltages indicate a forward fault, as shown in Fig. 41 and Fig. 42 for both terminals.
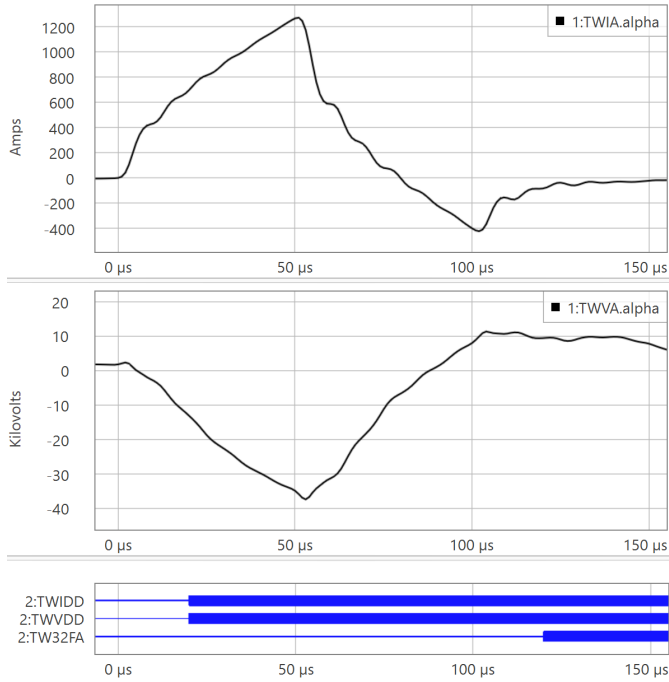
Fig. 42.   Navarro A-phase alpha-mode current and voltage TWs and digital bits operating times.

From Fig. 43 and Fig. 44, we can observe the remote relay keying, scheme channel latency, and performance in both relays. Also note that using the TW32 element with a direct fiber channel can achieve faster POTT scheme operation.
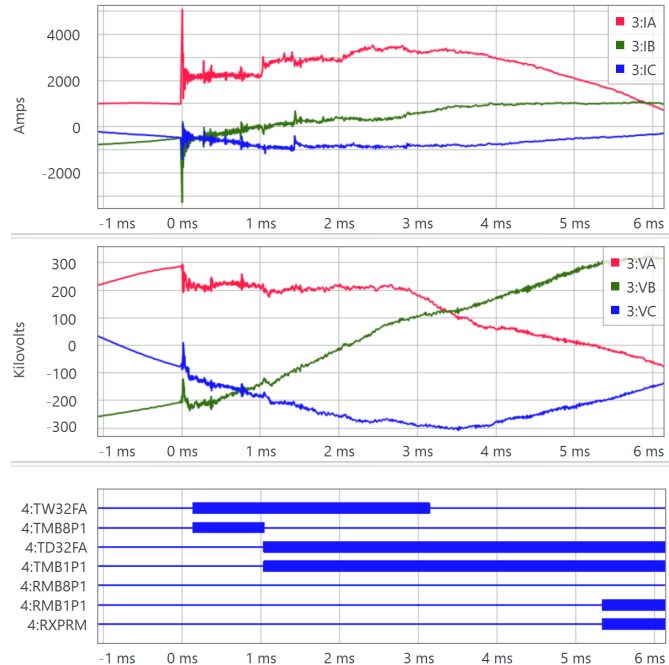
Fig. 43.   West Shackelford currents and voltages and POTT scheme operation.
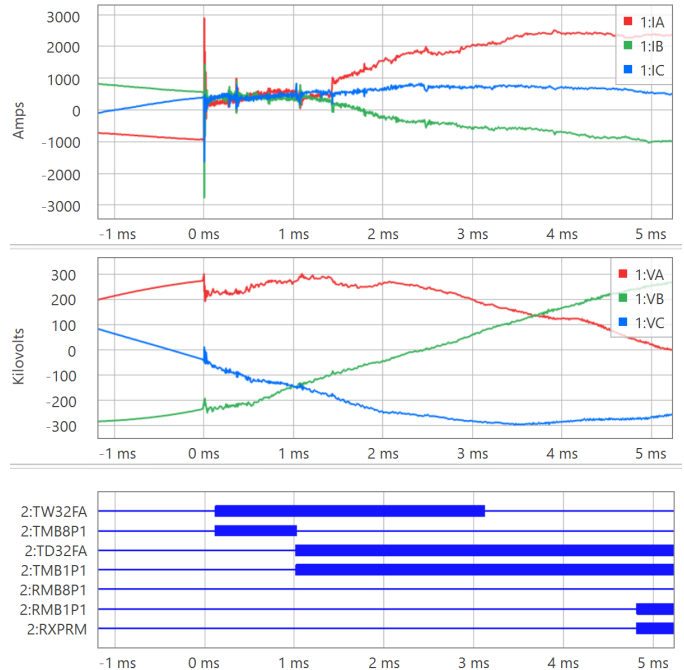
Fig. 44.   Navarro currents and voltages and POTT scheme operation.

Placing the POTT keying (TD32FA and TMB1P1) and POTT scheme receiver digital bits (RMB1P1) on the same time reference, as shown in Fig. 45, we can observe and measure the relay-to-relay channel latency. TMB1P1 (shown in blue) at West Shackelford asserts 4.0 ms before RMB1P1 for the POTT (RXPRM) scheme (shown in black) at Navarro, whereas TMB1P1 (shown in black) at Navarro asserts 4.1 ms before RMB1P1 for the POTT scheme (shown in blue) at West Shackelford. The 132 µs difference between the two POTT schemes is due to timing and the 100 µs processing interval of the UHS relays. The assertion time of 4.1 ms is also well below the 15 ms maximum allowable channel latency for the POTT scheme [3].
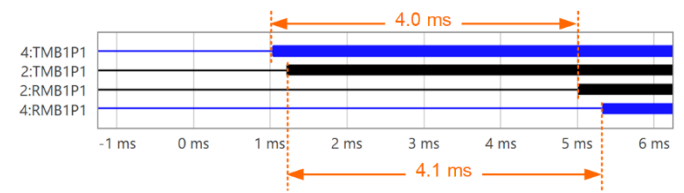
Fig. 45.   POTT keying and POTT scheme operation at West Shackelford (blue) and Navarro (black) showing relay-to-relay latency.

The C37.94 encoding has a transmit interval of 0.5 ms and requires 3 consecutive messages to be received and validated before the received digital bit asserts. This is 1.5 ms of the delay [3] for added security. As a result, the actual relay-to-relay channel latency during this fault was $4.1 - 1.5 = 2.6$ ms.

4)   TW-Based Fault Locating

The Bewley diagram in Fig. 46 shows the A-phase TW alpha-mode currents from West Shackelford and Navarro. The diagram helps to visualize the TWs from the fault and verify the DETWFL result. As shown in the figure, the fault location is 94.031 mi from West Shackelford and 130.869 mi from Navarro. Fig. 46 also shows that the initial TWs that arrived at each terminal have the same polarity (positive) and are

separated by less than the line's TWLPT of 1,232.13 μs. Operations confirmed that a lightning strike occurred at the same location and time (Tower Structure F 246 at 12:39:44.662 p.m. local time) as the fault observed by the UHS relays. Operations used data from DTN's WeatherSentry® Utility Edition software application that provides an archived lightning layer with time and date stamps on each lightning strike.
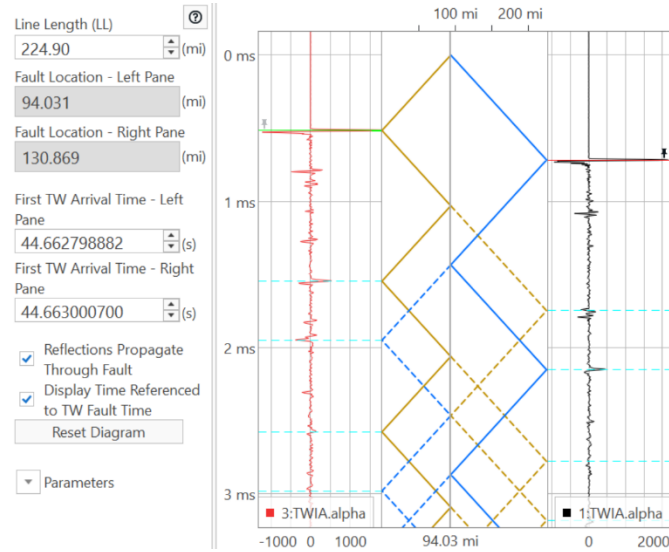
Fig. 46.   Bewley diagram showing A-phase alpha-mode current TWs for West Shackelford (red) and Navarro (black).

C.   Internal BG Fault at 18:38:20 UTC on May 11, 2021

On May 11, 2021, just less than 59 minutes after the fault described in Section V. B., a BG fault was recorded by the UHS relays monitoring the West Shackelford to Navarro 345 kV 224.9 mi transmission line (Line 1).

1)   Relay Operating Time

Shown in Fig. 47, at West Shackelford, the POTT scheme operated in 5.10 ms and TD32F asserted in 1.10 ms. TW32F and TD21BG did not assert.
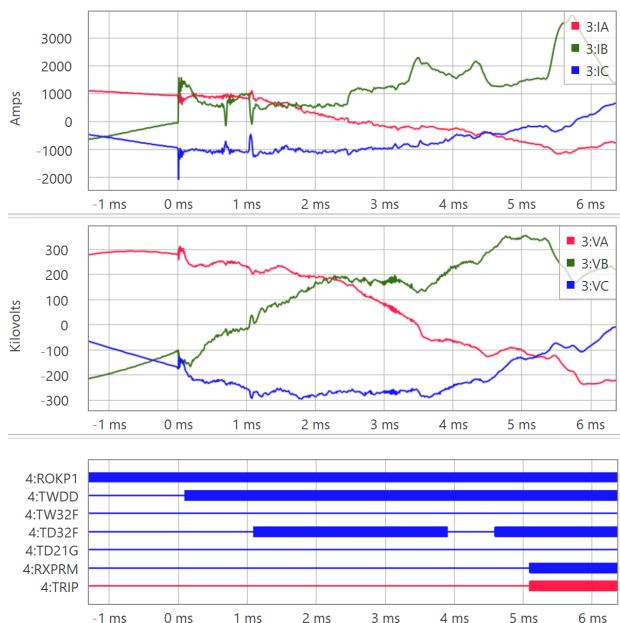
Fig. 47.   West Shackelford currents and voltages and digital bits operating times.

Shown in Fig. 48, at Navarro, the POTT scheme operated in 5.48 ms, TD32F asserted in 1.08 ms, and TD21BG asserted in 6.08 ms. Note that TW32F did not assert.
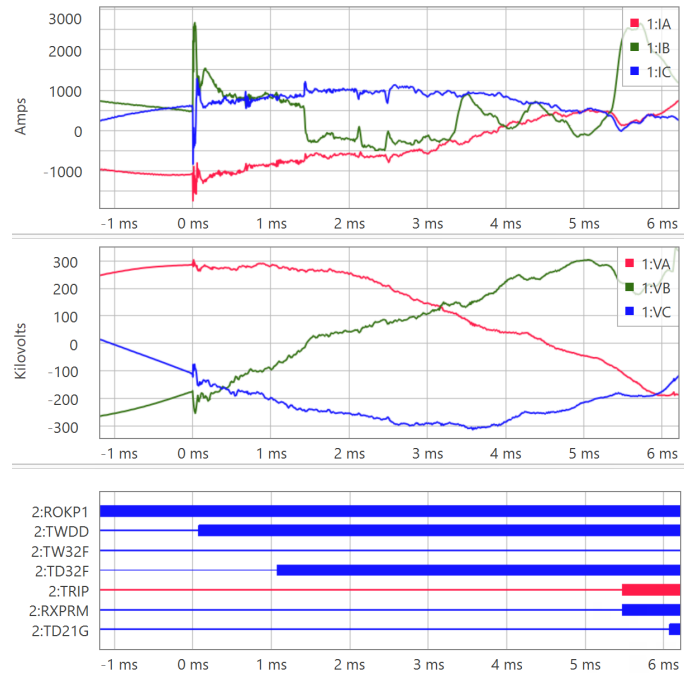
Fig. 48.   Navarro currents and voltages and digital bits operating times.

2)   TD21 Element Performance

With a reach of 90 percent, TD21BG asserted at Navarro and declared a Zone 1 BG fault. The fault was located at 42.0 percent (94.422/224.90 pu) of the line length as measured from Navarro, well within the TD21 underreaching Zone 1 element reach. TD21BG asserted in 6.08 ms, as shown in Fig. 49.
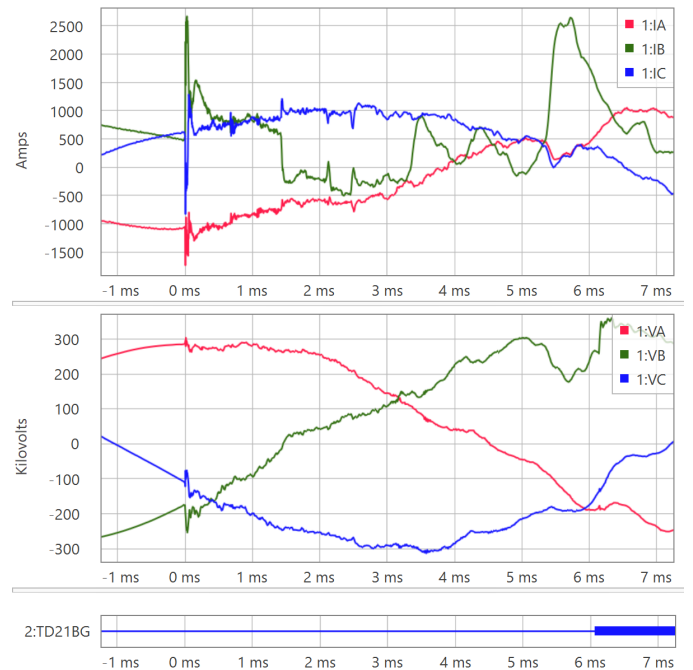
Fig. 49.   Navarro currents and voltages and TD21BG operating time.

From West Shackelford, the fault was located at 58 percent (1 – 0.420 pu) of the line length, well within the 90 percent reach of the TD21 element. However, as shown in Fig. 50, TD21BG restrained because the calculated VOP remained below the calculated VRT for the BG loop, prior to the TD21 element operating window expiring. In this case, we expect the TD21 element to restrain for the fault because the supervising incremental replica overcurrent (OC21BG) does not assert within the operating window. At 9 ms, when OC21BG does assert and VOP > VRT, the TD21 operating window has expired.
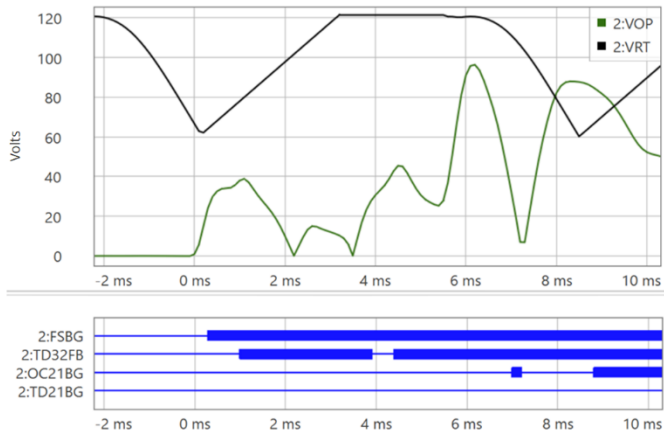
Fig. 50.   West Shackelford TD21BG restrains.

3)   POTT Scheme Performance
We observed that the TW32 element did not assert in either relay, even though a current TW disturbance was detected in both relays. From Fig. 51 and Fig. 52, we observe that the fault is in the forward direction for both terminals and both TWIDD and TWVDD asserted in both relays.
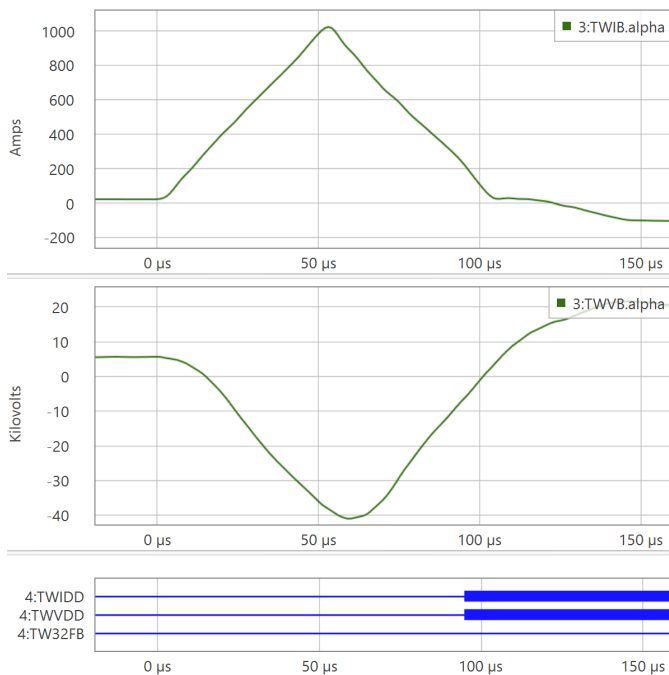
Fig. 51.   West Shackelford B-phase alpha-mode current and voltage TWs and digital bits.
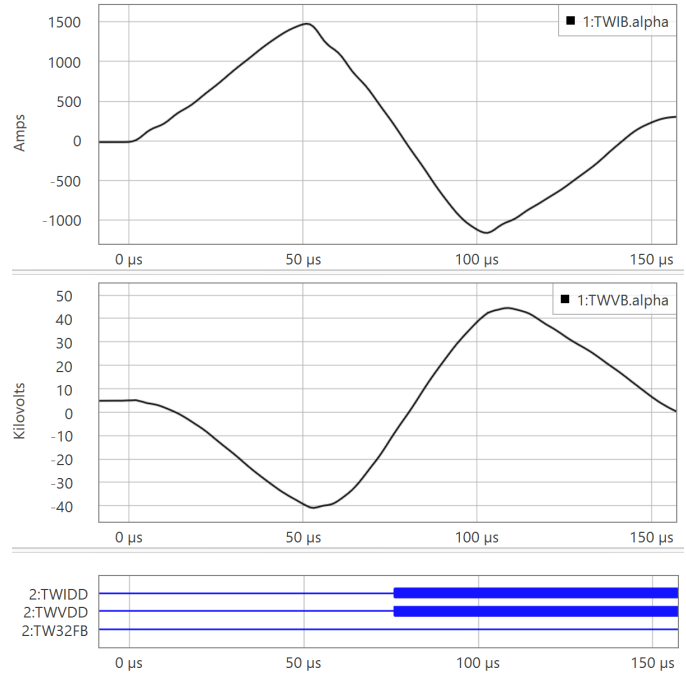
Fig. 52.   Navarro B-phase alpha-mode current and voltage TWs and digital bits.

From Fig. 53 and Fig. 54, we can observe the remote relay keying, scheme channel latency, and performance in both relays. Faster keying was not obtained because TW32FB (although setting ETW32 = Y) did not assert, and hence, TMB8P1 and KEYTW do not assert in the POTT scheme during this fault.
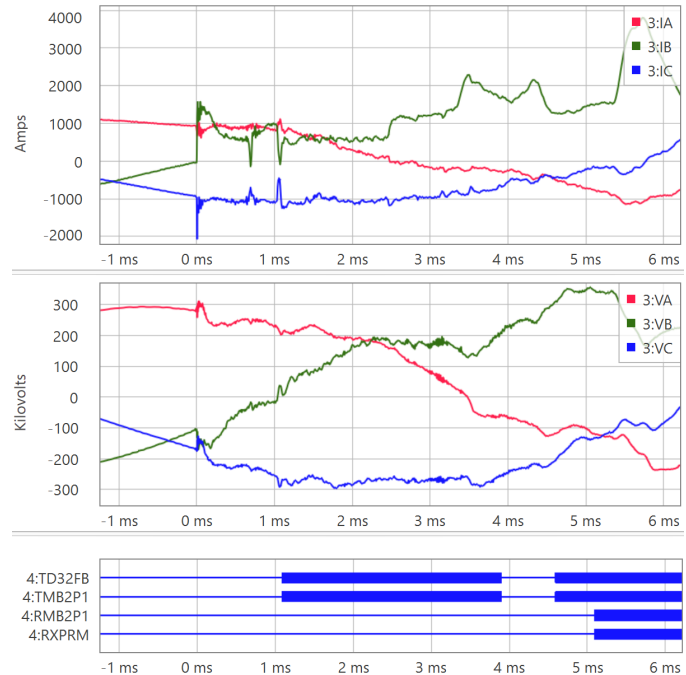
Fig. 53.   West Shackelford currents and voltages and POTT scheme operation.
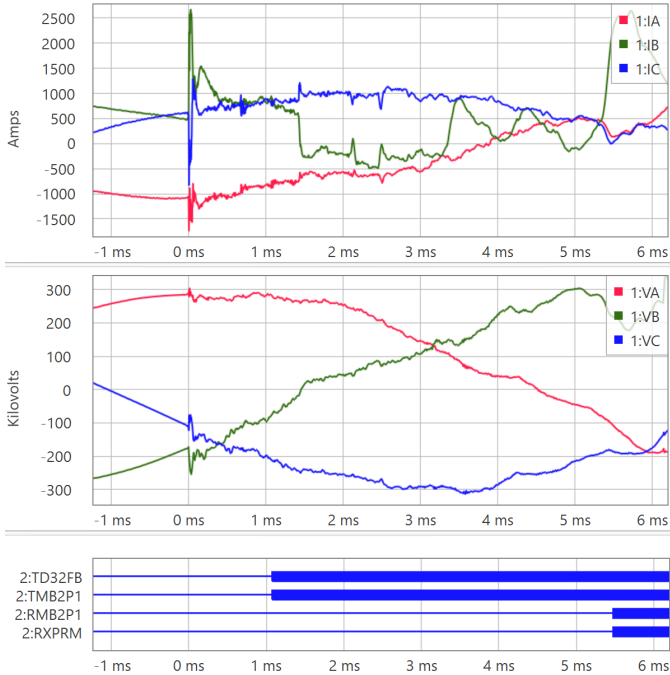
Fig. 54.   Navarro currents and voltages and POTT scheme operation.

Placing the POTT keying (TD32FB and TMB2P1) and POTT scheme receiver digital bits (RMB2P1) on the same time reference, as shown in Fig. 55, we can observe and measure the relay-to-relay channel latency. TMB2P1 (shown in black) at Navarro asserts 4.2 ms before RMB2P1 for the POTT (RXPRM) scheme (shown in blue) at West Shackelford, whereas TMB2P1 (shown in blue) at West Shackelford asserts 4.2 ms before RMB2P1 for the POTT scheme (shown in black) at Navarro. As a result, for reasons explained in Section V. B., the actual relay-to-relay channel latency during this fault was 4.2 – 1.5 = 2.7 ms.
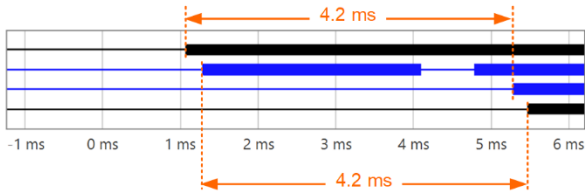
Fig. 55.   POTT keying and POTT scheme operation at West Shackelford (blue) and Navarro (black) showing relay-to-relay latency.

4)   TW-Based Fault Locating and Line Monitoring

The Bewley diagram in Fig. 56 shows the B-phase TW alpha-mode currents from West Shackelford and Navarro. The UHS relays located the fault at 130.478 mi from West Shackelford and 94.422 mi from Navarro. Fig. 56 also shows that the initial TWs that arrived at each terminal have the same polarity (positive) and are separated by less than the line's TWLPT of 1,232.13 µs. Again, using the WeatherSentry software, operations confirmed that a lightning strike occurred at the same time and location as the fault location calculated by the UHS relays.
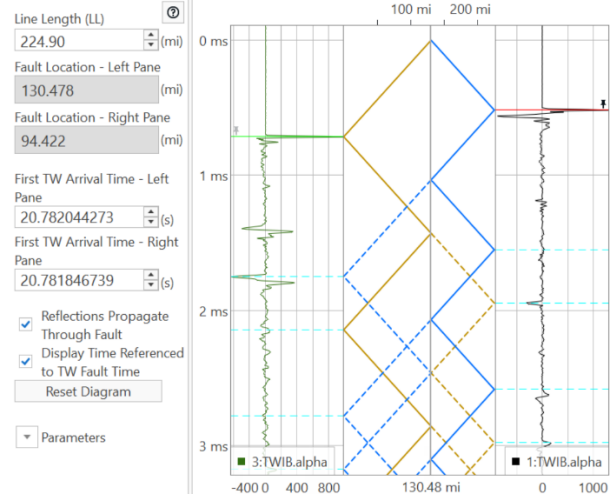
Fig. 56.   Bewley diagram showing B-phase alpha-mode current TWs for West Shackelford (green) and Navarro (black).
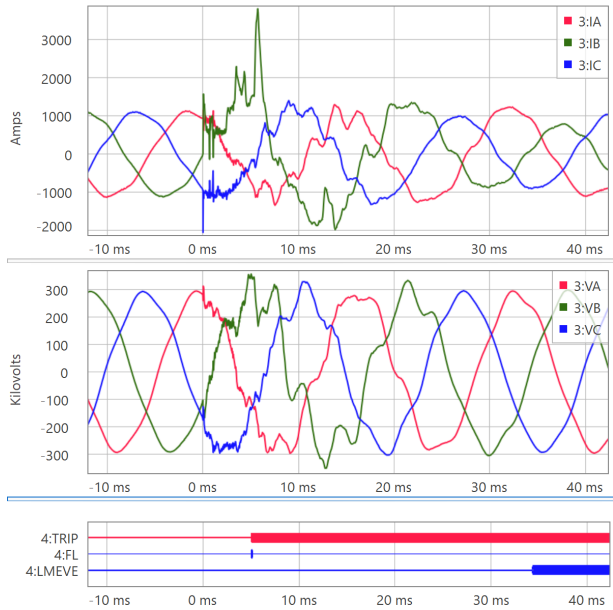
Fig. 57.   West Shackelford currents and voltages and line monitor event.
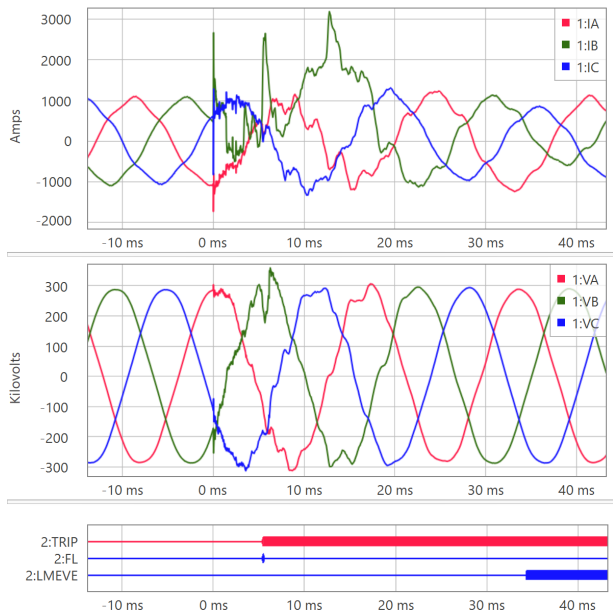
Fig. 58.   Navarro currents and voltages and line monitor event.

Using the DETWFL result, the line monitor in both UHS relays detected the fault, as shown with the assertion of the line monitoring digital bit (LMEVE) in Fig. 57 and Fig. 58. The line monitor then incremented the event count for the bins at 94.50 mi at Navarro and 130.50 mi at West Shackelford, respectively.

Fig. 59 shows the LINEMON.TXT file from the UHS relay at Navarro, which contains all the line monitor counters.

```
Line Monitoring History
Total number of events:       2
Location [mi]    Event Count
     0.25            0
     0.50            0
     0.75            0
     1.00            0
  …
    94.25            0
    94.50            1
    94.75            0
  …
   127.00            0
   127.25            1
   127.50            0
  …
   224.00            0
   224.25            0
   224.50            0
   224.75            0
```

Fig. 59.   Navarro line monitor data showing event counts.

D.   Summary

As the analysis of the transient event records for the three internal faults above detailed, Lone Star is observing expected UHS protection relay operating time performance, TWFL accuracy to one tower span, and line monitoring data on the 345 kV transmission network.

VI.   Conclusion

The UHS relays [3] have been installed to evaluate their protection elements and schemes (monitoring mode and nontripping) and to provide transient recording, fault locating (operational) and line monitoring (operational). The experience and observations through testing and field events were valuable and confirmed for Lone Star that these relays are secure, improve fault locating accuracy, and will improve the overall protection once applied for fault clearing for these two key series-compensated transmission lines.

Lone Star and other UHS relay users are routinely using time-synchronized protection test sources for field testing of UHS relays with protection speed communications schemes [12]. Utility testing technicians and engineers are already familiar with the testing equipment, related software tools, and testing requirements for phasor-based relay end-to-end testing. Applying UHS relays and using a TW injector during end-to-end testing is a manageable change in order to adopt the benefits UHS relays offer.

VII.   Acknowledgment

The authors gratefully acknowledge the contributions of Noe Encarnacion, Sergio Moriel, and Scott Cooper who assisted with the testing work and review of this document and Greg Smelich for his assistance with this document.

VIII.   References

[1] P. Kundur, *Power System Stability and Control*, McGraw-Hill Education, New York, NY, 1994, p. 636.

[2] E. Clark, J. Holbach, and S. Ward, "Real Time Simulation Testing of Complex Protection Schemes – A Case Study," proceedings of the 40th Annual Western Protective Relay Conference, Spokane, WA, October 2013.

[3] *SEL-T400L Time-Domain Line Protection Instruction Manual*. Available: selinc.com.

[4] F. Shanyata, S. Sharma, D. Joubert, R. Kirby, and G. Smelich, "Evaluation of Ultra-High-Speed Line Protection, Traveling-Wave Fault Locating, and Circuit Breaker Reignition Detection on a 220 kV Line in the Kalahari Basin, Namibia," proceedings of the 48th Annual Western Protective Relay Conference, Spokane, WA, October 2021.

[5] C. Pritchard, T. Hensler, N. Fischer, and B. Kasztenny, "Testing Superimposed-Component and Traveling-Wave Line Protection," proceedings of the 44th Annual Western Protective Relay Conference, Spokane, WA, October 2017.

[6] E. Schweitzer, III, A. Guzmán, M. V. Mynam, V. Skendzic, B. Kasztenny, and S. Marx, "Locating Faults by the Traveling Waves They Launch," proceedings of the 40th Annual Western Protective Relay Conference, Spokane, WA, October 2013.

[7] A. Sivesind, F. Sanchez, S. Cooper, and F. Elhaj, "Traveling Wave Relay Application, Commissioning, and Initial Experience," proceedings of the 72nd Annual Conference for Protective Relay Engineers, College Station, TX, March 2019.

[8] E. O. Schweitzer, III, B. Kasztenny, and M. V. Mynam, "Performance of Time-Domain Line Protection Elements on Real-World Faults," proceedings of the 42nd Annual Western Protective Relay Conference, Spokane, WA, October 2015.

[9] H. Moradi, D. Marquis, K. Garg, G. Smelich, and Y. Tong, "Testing and Commissioning Ultra-High-Speed Line Protection on a 345 kV Transmission Line," proceedings of 72nd Annual Conference for Protective Relay Engineers, College Station, TX, March 2019.

[10] *SEL-T401L Ultra-High-Speed Line Relay Instruction Manual*. Available: selinc.com.

[11] H. Moradi, K. Garg, M. V. Mynam, E. Chua, and J. Bell, "PNM Approach to Protecting Overcompensated High-Voltage Lines," proceedings of 72nd Annual Conference for Protective Relay Engineers, College Station, TX, March 2019.

[12] Field Experiences With Traveling-Wave Protection and Fault Locating. Available: selinc.com/TW-Field-Experiences.

[13] B. Kasztenny, M. V. Mynam, T. Joshi, and D. Holmbo, "Preventing Line Faults With Continuous Monitoring Based on Current Traveling Waves," proceedings of the 15th International Conference on Developments in Power System Protection, Liverpool, United Kingdom, March 9–12, 2020.

[14] B. Kasztenny, M. V. Mynam, "Line Length and Fault Distance Considerations in Traveling-Wave Protection and Fault-Locating Applications." Available: selinc.com.

IX.   Biographies

Matthew J. Lewis is a senior protection and control engineer at Lone Star Transmission, LLC in Mansfield, Texas. His current focus is maintenance and engineering of new generation interconnect projects. He is a registered Professional Engineer in Florida and Texas. He has 14 years of experience in electrical engineering with 9 of those years in electric power engineering. He received a BS in electrical engineering from Florida Atlantic University in Boca Raton, Florida, in 2008, and in 2016, he earned his Master of Engineering in electrical engineering, with emphasis on Industrial Power Systems, from the University of Houston in Houston, Texas.

Faris M. Elhaj is a training and application engineer at OMICRON electronics Corp., based in Houston, Texas. His current focus is on developing testing solutions for utility protection and control (P&C) applications including digital substations. He has 10 years of experience in electric power engineering, ranging from delivering training on P&C concepts to conducting commissioning activities for utilities and industrial plants. He received his Bachelor's and Master's degrees in electrical engineering from McMaster University in Hamilton, Ontario, Canada in 2007 and 2011.

Richard D. Kirby is a senior engineer at Schweitzer Engineering Laboratories, Inc. (SEL) in Houston, Texas. His current focus is metering systems, transient recording, and disturbance detection. He is a registered Professional Engineer in Arkansas, Louisiana, Michigan, Oklahoma, and Texas. He has 30 years of diverse electric power engineering experience. He received a BS in engineering from Oral Roberts University in Tulsa, Oklahoma, in 1992, and in 1995, he earned his Master of Engineering in electric power from Rensselaer Polytechnic Institute in Troy, New York. He is a senior member of the IEEE Power & Energy Society and the Industrial Applications Society.